66–14,225

LYNCH, Robert Hugh, 1925–

THE EFFECTS OF GAS HEATING AND VOLUME RECOMBINATION ON ELECTRON DENSITY PROFILES IN THE POSITIVE COLUMN.

The University of Oklahoma, Ph.D., 1966
Physics, electronics and electricity

University Microfilms, Inc., Ann Arbor, Michigan

THE UNIVERSITY OF OKLAHOMA

GRADUATE COLLEGE

THE EFFECTS OF GAS HEATING AND VOLUME RECOMBINATION ON ELECTRON DENSITY PROFILES IN THE POSITIVE COLUMN

A DISSERTATION

SUBMITTED TO THE GRADUATE FACULTY

in partial fulfillment of the requirements for the

degree of

DOCTOR OF PHILOSOPHY

BY

ROBERT HUGH LYNCH

Norman, Oklahoma

1966

THE EFFECTS OF GAS HEATING AND VOLUME RECOMBINATION ON

ELECTRON DENSITY PROFILES IN THE POSITIVE COLUMN

APPROVED BY

R. S. Fowler

S. B. Corrigan

Jack C. Arthur

Arthur Bernhart

C. C. Li

DISSERTATION COMMITTEE

ACKNOWLEDGEMENTS

Since coming to the University of Oklahoma to do graduate work, the author has had a fruitful association with Professor R. G. Fowler through his many stimulating discussions of research problems in the field of gaseous electronics. The author is also indebted to Professor Fowler for his energetic encouragement during periods of great perplexity.

Thanks are also due Professor S. J. B. Corrigan, who generously donated many hours of his time to quiet and careful discussion of the author's problems.

Miss Susan Shannon has also helped with some of the typing during many hours of the night. On several occasions she even spent the twenty-fifth hour of the day on the work.

Finally, the author thanks the personnel of the computer laboratory of the University of Oklahoma for processing his problem and enduring occasional complaints that the computer was confused.

TABLE OF CONTENTS

LIST OF TABLES

LIST OF ILLUSTRATIONS

CHAPTER I

INTRODUCTION AND SUMMARY

It is well known that in steady-state glow discharges in tubes the positive column tends to fill the entire cross-section at low gas pressures and currents because of the ambipolar diffusion process. The simplest example of this behavior was worked out by Schottky for a positive column consisting only of electrons, one species of ion, and the parent gas at a uniform temperature.[1] The well-known result of his investigation in the case of a cylindrical discharge is a radial profile of electron density given by the zeroth order Bessel function.

For many years since Schottky's work, deviations from this "normal" profile have been investigated both theoretically and experimentally. Although a wide variety of situations have been considered, the most important can be grouped into three classes:

(1) Those occurring in noble and electropositive gases at moderate currents and relatively high pressure;

(2) Those occurring at much lower currents and pressures in electronegative gases;

(3) Magnetic pinches occurring at low pressures and high currents.

Deviations from the normal distribution have also been studied experimentally for the case where a short D.C. pulse is passed through a noble gas during a time of about one msec. The resulting positive column has been found to constrict at moderate current densities

(order of 0.2 amp./cm.^{2}) and relatively low pressures (order of 10 mm. Hg).[3] Some unsuccessful attempts have been made by the author (R. H. Lynch) to explain the observations, assuming that the column had reached a steady state. A possible alternative explanation is that the column was in a transient state due to thermal instability.[4]

There are a few investigations which show that one cannot expect prounced variations to occur at low pressures and currents in noble gases. For very small currents where free diffusion predominates, theory predicts only a moderate wall-dependent constriction, which should change into the normal profile as the current is increased.[53]

Another situation has been investigated in which both direct and second-stage ionization take place.[6] If the second stage ionization predominates, the electron production term in the particle balance equation may vary quadratically with the electron density, and a constriction should occur. Spenke's result, however, was small and illustrated the fact that a precipitate radial decrease in ionization rate per electron is required in order to make the radial profile of electron density deviate appreciably from Schottky's solution. This fact was also shown for another case by Fabrikant.[7] He showed that if volume recombination between electrons and ions is appreciable, there is a radial increase in the net electron production rate per electron, which engenders only a small broadening of the radial profile.

Constrictions of the positive column in electronegative gases have been dealt with both experimentally and theoretically. In Woolsey's experiment[8], for example, a wall-dependent constriction was obtained at low currents and relatively low pressure. The constriction became

wall-independent as the current was increased. There were also characteristic variations in electric field strength, which were theoretically predicted for a model consisting of electrons, positive and negative ions, and the parent gas.[9,10]

The first of the above classes of situations are usually associated with gas heating. Much experimental and theoretical work has already been done on constrictions in high pressure arcs, where the electron temperature is nearly the same as the gas temperature.[11-15] The effect of gas heating in glow discharges has been recently investigated theoretically for a model consisting only of electrons, one kind of positive ion, and the parent gas. The result obtained was a radial profile which broadened as the heating increased.[16]

The main purpose of the investigation reported herein is to analyze theoretically a model consisting of a heated noble gas, its atomic and molecular ions, and electrons. After the basic theory of the gas-heated positive column is developed in Chapters II and III, Chapters IV and V are devoted to a brief analysis of two special situations in the positive column without volume recombination, and the constriction caused by gas heating and volume recombination is dealt with in Chapter VI.

CHAPTER II

BASIC THEORY OF THE POSITIVE COLUMN

It is assumed that the reader already has some knowledge of the kinetic theory of electrons and ions and is familiar with the papers on that subject.[17] In particular, a familiarity with the solution of the Boltzmann equation by expansion methods is assumed.[17-20] However, for convenience it is briefly outlined below for the steady state.

If the electron drift velocity is small as compared to the root mean square velocity, one can expand the electron phase density $f(\underline{r},\underline{v})$ in terms of spherical harmonics in velocity space:

$$f(\underline{v}) = f_{00}(v) + f_{10}(v)P_{10}(\theta) + f_{11}(v)P_{11}(\theta)\cos\phi + g_{11}(v)P_{11}(\theta)\sin\phi + \cdots, \tag{2.1}$$

where $f_{00}(v)$ is the isotropic part of the velocity distribution and the first order terms are small compared to it. In (2.1) and in what follows the dependence of quantities on $\underline{r}$ is implied. Because of the orthogonality of the spherical harmonics, only the isotropic term contributes to averages of scalar quantities $s(v)$; i.e., if the velocity distribution function is normalized to the electron concentration n, then we have

$$n\bar{s} \equiv \int f(\underline{v})s(v)\,d\underline{v} = 4\pi\int_0^\infty v^2 f_{00}(v)s(v)\,dv, \tag{2.2}$$

where $d\underline{v}$ is the three-dimensional volume element in velocity space. Likewise, since the velocity is a vector sum of only first order spherical harmonics, only the first order terms in (2.1) contribute to the average value of $\underline{v}s(v)$:

$$n\overline{s(v)\underline{v}} = \int f(\underline{v})\underline{v}\, s(v)d\underline{V} = \frac{4\pi}{3}\int_0^\infty v^3 s(v)\underline{f}_1(v)dv, \qquad (2.3)$$

where $\underline{f}_1 = \hat{i}f_{11} + \hat{j}g_{11} + \hat{k}f_{10}$, and has the direction of flow of the quantity $s(v)$.

Consider the steady state Boltzmann equation,

$$\underline{v}\cdot\nabla_r f + \underline{a}\cdot\nabla_v f = \frac{\partial_c f}{\partial t} + \frac{\partial_e f}{\partial t}. \qquad (2.4)$$

The right hand terms in this equation stand for the rates of change of f due to elastic and inelastic collisions, respectively, while $\nabla_r f$ is the spatial gradient and $\nabla_v f$ is the velocity gradient of f on the left side. The vector $\underline{a}$ is the electron acceleration. If we operate on the expansion (2.1) with the terms of (2.4), we obtain an infinite set of "Boltzmann equations" of different orders. Thus, an equation of order (ℓ,m) consists of those terms that are multiplied by $P_{\ell m}(\theta)$ and either the $\sin(m\phi)$ or the $\cos(m\phi)$. The number of equations that one derives equals the number of coefficients retained in the series (2.1). Higher order coefficients contained in these equations are neglected. Hence, if we retain the isotropic and the three first order terms, we get the zeroth order equation,[17]

$$\frac{1}{3}v\nabla_r\cdot\underline{f}_1 + \frac{1}{3v^2}\frac{\partial}{\partial v}\left(v^2\underline{a}\cdot\underline{f}_1\right) = \frac{m}{M}\frac{1}{v^2}\frac{\partial}{\partial v}\left[v^3\nu_c\left(f_{oo} + \frac{KT_g}{mv}\frac{\partial f_{oo}}{\partial v}\right)\right]$$
$$+ w(v) - \sum_e \nu_e(v)f_{oo}(v), \qquad (2.5)$$

and the first order vector equation,

$$\underline{f}_1 = -\frac{v}{\nu_c}\nabla_r f_{oo} - \underline{a}\,\frac{1}{\nu_c}\frac{\partial f_{oo}}{\partial v} . \qquad (2.6)$$

In equations (2.5) and (2.6) m/M is the ratio of electron mass to molecular mass, and ν_c and ν_e are the electron momentum transfer frequency and excitation frequencies respectively. The gas temperature in (2.5) is indicated by T_g. These equations apply only to the steady state with electric field and do not include terms for the interaction between electrons. These terms were obtained by J. H. Cahn in 1949[21,22] and are discussed in Appendix I.

In the zeroth order equation (the plasma balance equation) the first term on the left produces an effect on the shape of $f_{oo}(v)$ due to the spatial divergence of the electrons. The effect of force fields on $f_{oo}(v)$ is given by the second term. Since the magnetic field is assumed to be negligible, the acceleration is given by the equation,

$$\underline{a} = -\,e\underline{E}/m. \qquad (2.7)$$

The electric field induces a general drift of electrons away from the origin in velocity space. The opposite tendency, due to elastic collision energy loss, is represented by the first term on the right side of (2.5), while the effect on $f_{oo}(v)$ due to inelastic collisions is given by the last two terms. The term $\sum_e \nu_e f_{oo}$ gives the rate of disappearance of electrons in the "inelastic sink" while the term $w(v)$ gives the corresponding appearance rate of the inelastically scattered electrons in the vicinity of the origin in velocity space.

From equation (2.6) one obtains the effect of the concentration gradient and the force field on the flow rate of various quantities.

From the plasma balance equation one obtains various conservation equations by taking velocity averages of the respective terms with respect to appropriate weight functions. Similar operations on the first order equation give flow or diffusion equations.

The simplest case to consider is that where the spatial variation of gas density and electron temperature can be neglected. In that case neither ν_c nor ν_e vary with position. Experiments on the variation of mean electron energy with E/p indicate that for moderate electron densities ($n \sim 10^{11}/cm.^3$) we can also assume that inelastic collisions have little effect on the velocity distribution profile as long as the average electron energy is small as compared to the excitation energy.[23] Hence, we can assume that

$$f_{oo}(\underline{r},v) = A(\underline{r}) \exp.(-\beta^2 v^2), \tag{2.8}$$

and calculate velocity averages accordingly. This case (constant gas density) was analyzed and experimentally studied especially in the decade before World War II.[24]

Since the effect of gas heating will be discussed later, the desired flow and conservation equations will be derived from (2.5) and (2.6) with spatially variable collision frequencies.

Macroscopic Equations

For a gas heating theory of the positive column we need the following macroscopic equations for positive ions, electrons, and neutral molecules:

(1) Particle conservation

(2) Energy conservation

(3) Particle flow

(4) Energy flow

To obtain the particle flow equation for electrons, we multiply (2.6) by $4\pi v^3/3$ and integrate to obtain the equation,

$$\frac{4\pi}{3}\int_0^\infty v^3 \underline{f}_1 dv = -\frac{4\pi}{3}\int_0^\infty \frac{v^4}{\nu_c}\nabla_r f_{oo}\, dv - \underline{a}\frac{4\pi}{3}\int_0^\infty \frac{v^3}{\nu_c}\frac{\partial f_{oo}}{\partial v} dv . \qquad (2.9)$$

Since $$f_{oo}(\underline{r},v) = A(\underline{r}) \exp.(-\beta^2 v^2),$$

then, $$\frac{\partial f_{oo}}{\partial v} = -2\beta^2 v f_{oo}, \qquad (2.10)$$

where $A = n(\beta/\sqrt{\pi})^3$ and $\beta^2 = m/2kT$.

Then, the last term in (2.9) reduces to the expression $\mu n\underline{E}$, where the electron mobility μ is the velocity average,

$$\mu = \frac{e}{kT}\frac{1}{3}\overline{(v^2/\nu_c)} . \qquad (2.11)$$

The first term on the right side of (2.9) can be simplified by factoring out the position dependence of ν_c. That is, let

$$\nu_c(v,\underline{r}) = N(\underline{r})\, v\sigma_c(v) \equiv N(\underline{r})\,\nu_o(v), \qquad (2.12)$$

where ν_o is the elastic collision frequency for unit gas density (N = 1 molecule/cm.^{3}). Hence, the term becomes

$$-\frac{4\pi}{3}\frac{1}{N}\int_0^\infty \frac{v^4}{\nu_o}\nabla_r f_{oo}(\underline{r},v)\, dv = -\frac{1}{N}\nabla_r(nD_o), \qquad (2.13)$$

where $D_o = (1/3)\overline{(v^2/\nu_o)}$ is the electron diffusion coefficient in a gas of unit density.

From the definition (2.3) of $n\overline{s\underline{v}}$ it follows that the term on the left side of (2.9) is merely

$$n\,\underline{\bar{v}} \equiv \underline{\Gamma}, \qquad (2.14)$$

the particle current density. Hence, the diffusion equation finally becomes

$$\underline{\Gamma} = -\frac{1}{N}\nabla_r(nD_o) - \frac{\mu_o}{N} n\underline{E}, \tag{2.15}$$

where μ_o is the electron mobility for unit gas density.

The heat flow equation is similarly obtained from (2.6) by letting $s(\underline{r},v)$ in the definition of $n\overline{s\underline{v}}$ be the particle kinetic energy $\frac{1}{2}mv^2$. That is, we multiply (2.6) by $2\pi mv^5/3$ and integrate it term by term. The result is

$$\underline{q} \equiv \tfrac{1}{2} nm\overline{v^2\underline{v}} = -\frac{1}{N}\nabla_r(nd_o) - \frac{H_o}{N} n\underline{E}, \tag{2.16}$$

where

$$d_o = \frac{m}{6}\overline{(v^4/\nu_o)},$$

$$H_o = \frac{m}{6}\frac{e}{kT}\overline{(v^4/\nu_o)},$$

and $\underline{q}$ is the heat current density.

The particle and energy conservation equations are obtained from (2.5). In view of the definition of $n\bar{s}$ in terms of f_{oo}, we multiply (2.5) by $4\pi v^2$ and integrate it term by term over v to get the equation

$$\int_0^\infty \frac{4\pi}{3} v^3 \nabla_r\cdot\underline{f}_1 dv + \int_0^\infty \frac{4\pi}{3}\frac{\partial}{\partial v}(v^2\underline{a}\cdot\underline{f}_1)dv = \tag{2.17}$$

$$= \frac{4\pi m}{M}\int_0^\infty \frac{\partial}{\partial v}\left[v^3\nu_c\left(f_{oo} + \frac{kT_g}{mv}\frac{\partial f_{oo}}{\partial v}\right)\right]dv + 4\pi\int_0^\infty v^2\left[w(v) - f_{oo}\sum_e \nu_e(v)\right]dv.$$

If we take the divergence operator outside the integral in the first term we get the term $\nabla_r\cdot\underline{\Gamma}$. The next two terms vanish because $v^2\underline{f}_1$ and

$$v^3\nu_c\left(f_{oo} + \frac{kT_g}{mv}\frac{\partial f_{oo}}{\partial v}\right)$$

both vanish at the limits of integration. In the last term the integral over the source w(v) cancels out the integrals over all the excitation modes except ionization, since for every electron disappearing in the inelastic sink due to ionization, two appear in the source. That is,

$$4\pi\int_0^\infty v^2\left[w(v) - f_{oo}\sum_e \nu_e(v)\right]dv = 4\pi\int_0^\infty v^2 f_{oo}\,\nu_i(v)dv = n\bar{\nu}_i \,. \qquad (2.18)$$

So we obtain the particle conservation equation,

$$\nabla_r\cdot\underline{\Gamma} = n\bar{\nu}_i \equiv nN\bar{\nu}_{io} \,, \qquad (2.19)$$

where $\bar{\nu}_{io}(\underline{r})$ is the average frequency of direct ionization per electron in a gas of unit density.

In order to get the energy conservation equation, we now multiply (2.5) by $2\pi m v^4$ and integrate it term by term. As in the previous case, the first term gives the heat divergence $\nabla_r\cdot\underline{q}$. In the last term all modes of excitation make a contribution since for the eth mode of excitation (or ionization) the difference between the kinetic energies of the electron in the sink and the corresponding source electron is the excitation energy V_e. Therefore,

$$2\pi m\int_0^\infty v^4\left[w(v) - f_{oo}\sum_e \nu_e(v)\right]dv = -n\sum_e V_e\bar{\nu}_e \,. \qquad (2.20)$$

In the energy conservation equation the two middle terms are not zero. For the second term we get, integrating by parts,

$$\int_0^\infty \frac{2\pi}{3} m v^2 \frac{\partial}{\partial v}(v^2\,\underline{a}\cdot\underline{f}_1)\,dv = \frac{2\pi}{3} m v^4\,\underline{a}\cdot\underline{f}_1\Big|_0^\infty - \frac{4\pi m}{3}\int_0^\infty v^3\,\underline{a}\cdot\underline{f}_1\,dv$$

$$= -m\underline{a}\cdot\underline{\Gamma} = -e\underline{E}\cdot\underline{\Gamma} \,, \qquad (2.21)$$

since $\underline{f}_1 v^4$ vanishes at both limits. Integration by parts likewise gives for the elastic collision term,

$$2\pi \frac{m^2}{M} \int_0^\infty v^2 \frac{\partial}{\partial v}\left[v^3 \nu_c \left(f_{oo} + \frac{kT_g}{mv} \frac{\partial f_{oo}}{\partial v} \right) \right] dv = -4\pi \frac{m^2}{M} \int_0^\infty v^4 \nu_c \left(f_{oo} + \frac{kT_g}{mv} \frac{\partial f_{oo}}{\partial v} \right) dv$$

$$= -\frac{2m}{M} n \overline{(1/2\, mv^2 \nu_c)} - \frac{m}{M} kT_g n \overline{\left(v \nu_c \frac{1}{f_{oo}} \frac{\partial f_{oo}}{\partial v} \right)} . \qquad (2.22)$$

In the first term of this expression 2m/M is the average fraction of kinetic energy transferred by an electron to a molecule not moving before the collision. Hence, this term gives the rate per unit volume at which electrons lose energy to a gas at absolute zero. The second term gives the rate at which the molecules at temperature T_g give back energy to the electrons. If f_{oo} is Maxwellian, the elastic collision expression reduces to

$$-n \frac{2m}{M} \overline{(1/2\, mv^2 \nu_c)} (1 - T_g/T) , \qquad (2.23)$$

The complete electron energy conservation equation is then

$$\nabla_r \cdot \underline{q} = -e\underline{E} \cdot \underline{\Gamma} - \frac{2m}{M} \overline{(1/2\, mv^2 \nu_c)} (1 - T_g/T) - n \sum_e V_e \bar{\nu}_e . \qquad (2.24)$$

This equation means that in the steady state, the rate of outflow of electron energy per unit volume equals the net rate of production of the energy per unit volume. The latter equals the rate at which the electric field does work on the electrons minus the rate of loss of electron energy due to elastic and inelastic collisions.

Since the electric field strength divided by gas pressure is

relatively small in the constriction phenomena of interest, the average energy gained from the field by a positive ion between collisions is much smaller than kT^+. That is, $eE\lambda^+/kT^+ \ll 1$, where λ^+ is the mean free path of the positive ions. For helium molecular ions $\lambda^+ \sim 10$ cm./p, where p is the gas pressure in dynes/cm.^{2}. Then, if $T^+ \sim 1000^\circ$ K. and $E/p \sim 10^{-7}$ statv.cm./dyne (see Chapter VI), we get the result,

$$eE\lambda^+/kT^+ \sim 10^{-3}.$$

Then the motion of the positive ions can be described by a diffusion equation with the same form as (2.15); i.e.,

$$\underline{\Gamma}^+ = -\frac{1}{N}\nabla_r(n^+ D_o^+) + \frac{\mu_o^+}{N} n^+ \underline{E}\ , \tag{2.25}$$

where the coefficients have the same empirical definitions as before but are not calculated from the same velocity averages.[25]

From the point of view of energy conservation and energy flow, the positive ions can be considered as identical with the neutrals. Since the electric field is not strong and the energy exchange rate between ions and neutrals is large, the energy conservation equation for the ions reduces to

$$T^+ = T_g. \tag{2.26}$$

Also, the heat conduction due to the ions is negligible because we assume that $n^+ \ll N$.

If the inelastic interactions going on are only ionization and excitations of neutrals by electrons, the particle conservation equation is the same for ions as for electrons; i.e.,

$$\nabla_r \cdot \underline{\Gamma}^+ = n\bar{\nu}_i\ . \tag{2.27}$$

As a result, the radial components of the electron and ion current densities are equal, and if the axial electron density is sufficiently large, ambipolar diffusion predominates in the positive column. In cylindrical geometry a criterion[5] for this condition is

$$\frac{3kT\bar{\nu}_i\, J_1^+}{4\pi e^2 D_a n_0 J_0^5} \ll 1,$$

where $J_0(r\sqrt{\bar{\nu}_i/D_a})$ and $J_1(r\sqrt{\bar{\nu}_i/D_a})$ are Bessel functions and

$$D_a = \frac{\mu^+}{\mu} D .$$

In this type of situation the solution of the diffusion equations (2.15) and (2.25) and Poisson's equation leads to the well known results:

$$\Gamma_r = -\frac{\mu^+}{\mu}\frac{1}{N}\frac{\partial}{\partial r}(nD_0), \tag{2.28}$$

$$E_r = -\frac{1}{\mu_0 n}\frac{\partial}{\partial r}(nD_0), \tag{2.29}$$

where E_r is the radial space charge field associated with ambipolar diffusion.

In the steady state the total pressure in the plasma is assumed to be uniform. Because of low specific ionization the partial electron pressure is very small (about .01 p) so the pressure of the neutrals is nearly constant. For the same reason, the drift velocity of neutrals from wall to axis is also slight. Hence, the diffusion equation and the particle balance equation for the neutrals reduce to

$$p = NkT_g = \text{const.} \tag{2.30}$$

In the derivation of the energy balance equation, it is assumed that the gas obtains all its thermal energy from elastic collisions with

the electrons and none from collisions of the second kind with excited atoms. Hence, we obtain

$$\nabla_r \cdot \underline{Q} = n(2m/M)\overline{(\tfrac{1}{2}mv^2 \nu_c)}(1 - T_g/T), \tag{2.31}$$

where the heat flow vector $\underline{Q}$ is given as

$$\underline{Q} = -\lambda \nabla_r T_g . \tag{2.32}$$

According to the Enskog theory, the heat conductivity λ is independent of pressure but nearly proportional to $T_g^{\frac{1}{2}}$ in the case of hard sphere collisions.[26]

We now have the equations needed for an analysis of the gas-heated positive column.

CHAPTER III

THE POSITIVE COLUMN WITH GAS HEATING

In what follows it is assumed there is only one type of positive ion. Hence, the equations of interest are (2.15), (2.16), (2.19), (2.24), (2.28), (2.29), (2.31), and (2.32). It is also assumed that no quantities vary with z, the axial coordinate and that no convection takes place.

The way in which the gas concentration occurs in these equations suggests the change of variable,

$$s = pr. \tag{3.1}$$

With this substitution and also equation (2.30), the macroscopic equations are as follows:

Electron conservation:

$$\nabla_s \cdot \underline{\Gamma} = \frac{n}{kT_g} \bar{\nu}_{io} . \tag{3.2}$$

Electron flow:

$$\underline{\Gamma} = - kT_g \nabla_s (nD_o) - kT_g \mu_o n \underline{E}_s , \tag{3.3}$$

where $\underline{E}_s = \underline{E}/p$.

Electron energy conservation:

$$\nabla_s \cdot \underline{q} = - e\underline{E}_s \cdot \underline{\Gamma} - \frac{2m}{M} \frac{n}{kT_g} \overline{(\tfrac{1}{2} m v^2 \nu_o)}(1 - T_g/T) - \frac{n}{kT_g} \sum_e V_e \bar{\nu}_{eo} . \tag{3.4}$$

Electron Energy flow:

$$\underline{q} = -kT_g \nabla_s (n d_o) - kT_g H_o n \underline{E}_s . \tag{3.5}$$

Ambipolar diffusion equations:

$$\underline{\Gamma}_r^+ = \underline{\Gamma}_r = -\frac{\mu^+}{\mu} kT_g \nabla_s (nD_o), \tag{3.6}$$

$$\underline{E}_{sr} = -\frac{1}{n\mu_o} \nabla_s (nD_o) . \tag{3.7}$$

Gas heating equations:

$$\underline{Q}_r = -\lambda(T_g) p \nabla_s T_g , \tag{3.8}$$

$$\nabla_s \cdot \underline{Q} = \frac{2m}{M} \frac{n}{kT_g} \overline{(\tfrac{1}{2} m v^2 \gamma_o)} (1 - T_g/T) . \tag{3.9}$$

In the above equations the gradient operator ∇_s refers to the maximum rate of change with respect to s.

From the definitions of the mobility and diffusion coefficients, it follows that

$$\begin{aligned} d_o &= ckTD_o, \\ H_o &= ckT\mu_o, \end{aligned} \tag{3.10}$$

where c is a slowly varying function of T.

There are three unknown quantities--the gas temperature, the electron temperature, and the electron concentration. The first of three simultaneous equations is derived by inserting the expressions (3.10) into (3.5) to get the radial part of the heat flow vector:

$$\underline{q}_r = -kT_g ckT \nabla_s (nD_o) - kT_g nD_o \nabla_s (ckT) - kT_g ckT\mu_o n \underline{E}_{sr}. \tag{3.11}$$

The radial space charge field is eliminated by comparing (3.11) with (3.3). The result is

$$\underline{q}_r = ckT\underline{\Gamma}_r - kT_g n D_o \nabla_s(ckT) . \tag{3.12}$$

We take the divergence of (3.12) in order to get the left side of (3.4):

$$\nabla_s \cdot \underline{q} = ckT\nabla_s \cdot \underline{\Gamma} + \underline{\Gamma} \cdot \nabla_s(ckT) - \nabla_s \cdot (kT_g n D_o \nabla_s(ckT)). \tag{3.13}$$

Inserting (3.2), (3.6), and (3.7) into (3.13), we obtain

$$\nabla_s \cdot \underline{q} = nc\bar{\nu}_{io}\frac{T}{T_g} - \frac{\mu^+}{\mu} kT_g \nabla_s(nD_o) \cdot \nabla_s(ckT) - \nabla_s \cdot (kT_g n D_o \nabla_s(ckT)). \tag{3.14}$$

Since the ratio $\mu^+/\mu \ll 1$, the second term on the right can be neglected. The first term on the right of (3.14) is also very small by comparison with the last term on the right of (3.4) because for the conditions of interest $kT \ll V_e$, and the total excitation frequency is larger than the ionization frequency. The right side of (3.4) is expanded with the help of (3.3), (3.6), and (3.7), and the definition

$$\overline{(\tfrac{1}{2} m v^2 \nu_o)} \equiv c'(T) kT. \tag{3.15}$$

Then, also inserting (3.14) into (3.4), we finally obtain the energy balance equation

$$\nabla_s \cdot (kT_g n D_o \nabla_s(ckT)) = -eE_{sz}^2 \mu_o kT_g n + e\frac{\mu_o^+}{\mu_o^2}\frac{kT_g}{n}\left[\nabla_s(nD_o)\right]^2 + \frac{2m}{M}\frac{T}{T_g} nc'(1 - T_g/T) + \frac{h}{kT_g}\sqrt{V_e}\,\bar{\nu}_{eo} . \tag{3.16}$$

The second term on the right side of (3.16) represents the rate of loss of electron energy caused by ambipolar drift of the electrons to the wall in opposition to the attractive force of the radial space charge field. It is shown in Appendix-II that this term is very small except very near the wall. The other terms on the right side of (3.16) represent a local balance at each point between the loss rate of energy due to collisions and the gain rate of energy due to the axial field component. In the gas-heated positive column this engenders a radial electron temperature variation that is more or less suppressed by the heat conduction process represented by the divergence term in (3.16).

The second simultaneous equation that is required is obtained from (3.2), (3.6), and (3.7). Theory[37] indicates that at temperatures well above 300° K. the atomic ion mobility in noble gases is the approximate function of gas temperature,

$$\mu_o^+ = \mu' T_g^{-\frac{1}{2}}, \tag{3.17}$$

where μ' is a constant. Inserting this expression into (3.6) and taking the divergence of the result, we obtain for (3.2):

$$\mu' k \nabla_s \cdot \left[\frac{T_g^{1/2}}{\mu_o} \nabla_s (n D_o) \right] = - \frac{n}{k T_g} \bar{\nu}_{io}(T). \tag{3.18}$$

The gas equations (3.8) and (3.9) yield the third simultaneous equation,

$$\nabla_s \cdot (\lambda \nabla_s T_g) = - \frac{2m}{M} \frac{T}{T_g} \frac{n}{P} c'(1 - T_g/T). \tag{3.19}$$

Of the three equations (3.16), (3.18), and (3.19), only the last one contains an explicit pressure dependence. This fact and the

definition of the radial variable s suggest that if the axial electron density n_o is varied with pressure (n_o/p held constant) and the tube radius R is varied inversely with pressure (pR held constant), then the shape of the radial profile of n stays constant and the radial profiles of T and T_g are also constant both with respect to shape and absolute magnitude. Since every term of (3.16) contains n, it is also true that E_{sz} does not vary in the above type of variation of pressure and radius. Then, according to (3.3), the axial component of current density at any point is proportional to pressure. Since the tube cross-sectional area varies inversely with p^2, the total tube current I varies inversely with p. It follows that the solution of (3.16), (3.18), and (3.19) gives n/n_o, T_g, and T as functions of s and the two parameters R' = pR and I' = pI.

Different situations arise in the column in different ranges of R'. If R' is very small, the derivative terms in (3.18) are relatively large and $\bar{\nu}_{io}$ has to be large in order to make up for the rapid diffusion of electrons to the wall. Then, T is large enough so that the energy loss due to inelastic collisions outweighs the elastic collision energy loss (see Chapter V). As a result, the local energy balance is maintained by the radially varying inelastic energy loss rate, and the corresponding radial variation of electron temperature is small.

As R' is increased, T decreases until the inelastic energy loss rate is negligible. For larger values of R' the radial variation of T depends upon a competition between the variation of the elastic collision energy loss rate and the electron heat conduction. If R' is still low enough, the heat conduction terms on the left side of (3.16) are large, and the radial variation of T engendered by the first and third

terms on the right side of (3.16) is suppressed (see Appendix III). As R' is increased still further, the heat conduction becomes ineffectual, and the radial variations of T_g and T are comparable. This results in a precipitate decrease of ionization rate from axis to wall.

These different cases will now be considered in some detail.

CHAPTER IV

THE POSITIVE COLUMN DOMINATED BY ELASTIC COLLISIONS

This situation has been recently investigated and definite results were obtained with a computer.[16] The author's analysis (without results) differs in detail from the analysis of Ecker and Zöller. Consequently, there may be a qualitative difference in the results. This depends on the assumptions that one makes about the variations of certain coefficients with the electron and gas temperatures. We now derive the relevant equations and explain the difference.

The effects of inelastic collisions and electron heat conduction are neglected. Hence, the energy balance equation (3.16) becomes

$$e E_{sz}^2 = \frac{2m}{M} \frac{c'}{k} \frac{T}{T_g^2} \frac{1}{\mu_o}, \tag{4.1}$$

where it is assumed that $T_g/T \ll 1$. The right side of (4.1) is uniform since the axial component of the field strength is assumed to be uniform. Therefore, we obtain the equation,

$$c'(T_o) \frac{T_o}{T_{go}^2} \frac{1}{\mu_o(T_o)} = c'(T) \frac{T}{T_g^2} \frac{1}{\mu_o(T)}, \tag{4.2}$$

or

$$T/T_o = (T_g/T_{go})^2 \frac{\mu_o(T)}{\mu_o(T_o)} \frac{c'(T_o)}{c'(T)}. \tag{4.3}$$

In these equations, T_{go} and T_o are the respective values of T_g and T on the axis.

Consider the special case where ν_o = const.x v. In that case,

$$c'(T) = \text{const.} \times T^{1/2},$$

$$\mu_o(T) = \text{const.} \times T^{-1/2}, \tag{4.4}$$

so (4.3) simplifies to

$$T/T_o = T_g/T_{go}. \tag{4.5}$$

Also for a Maxwellian distribution,

$$D_o/\mu_o = kT/e. \tag{4.6}$$

If (4.5) and the above expression (4.4) for the coefficient μ_o are inserted into (3.18), the equation,

$$\nabla_s^2 n = -Kn\bar{\nu}_{io}(T_g)T_g^{-5/2} - 1/2\, n\frac{\nabla_s^2 T_g}{T_g} - \frac{1}{4}n\left(\frac{\nabla_s T_g}{T_g}\right)^2 - 2\nabla_s n \cdot \frac{\nabla_s T_g}{T_g}, \tag{4.7}$$

is obtained, where K is a constant. The second term on the right side of (4.7) is associated with thermal diffusion. It can be related to simpler terms by means of the gas heating equation (3.19). To a fair approximation,

$$\lambda = \lambda' T_g^{1/2}; \quad \lambda' = \text{const.}$$

If we insert this formula into equation (3.19), we get the equation,

$$\nabla_s^2 T_g = - K' n - \tfrac{1}{2} (\nabla_s T_g)^2 / T_g , \qquad (4.8)$$

where K' is another constant. The right side of (4.8) is substituted for $\nabla_s^2 T_g$ in (4.7) to get

$$\frac{d^2 n}{ds^2} = - K n \bar{\nu}_{io} T_g^{-5/2} + \tfrac{1}{2} K' \frac{n^2}{T_g} - \frac{2}{T_g} \frac{dn}{ds} \frac{dT_g}{ds} - \frac{1}{s} \frac{dn}{ds} . \qquad (4.9)$$

There are two classes of profiles which one obtains by solving this equation and equation (4.8). One consists of profiles which go to zero for some value of s and hence can satisfy the boundary condition,

$$n(Rp) = 0,$$

at the wall. These profiles may be either broadened or constricted, depending on how K' compares with K. In Chapter VI is shown that the thermal diffusion term (second term on the right side of (4.9)) has a very weak effect. Therefore, the third term on the right side of (4.9) dominates the column after the ionization term has become negligible towards the wall. Since this term is increasingly negative towards the wall, it has a broadening effect on the radial profile.

The other class of profiles turn upwards either initially or at some point near the axis. That is, the ionization term is either less or just a little greater in magnitude than the thermal diffusion term on the axis. Away from the axis, the former quickly decreases, leaving the latter dominant. Then the grad n becomes positive, both the second and third terms on the right side of (4.9) become increasingly positive, and the profile cannot turn down to satisfy the boundary condition.

In their work,[16] Ecker and Zöller use the relations

$$T \propto T_g, \quad D_a \propto T_g^2, \quad \mu \propto T_g.$$

As equations (4.1) to (4.5) show, this simple relation between the electron and gas temperatures results if one assumes that $\nu_o \propto v$. In that case, the variation of electron mobility with gas temperature is $\mu = \mu_o/N \propto T_g^{\frac{1}{2}}$, and the corresponding variation of the electron diffusion coefficient is $D \propto T_g^{3/2}$. Then, the ambipolar diffusion coefficient is given by the relation,

$$D_a = \frac{\mu^+}{\mu} D = \frac{\mu_o^+}{N} \frac{kT}{e} \propto T_g^{3/2},$$

since $\mu_o^+ \propto T_g^{-\frac{1}{2}}$. Apparently, our results should agree at least qualitatively with those of Ecker and Zöller if we assume that μ_o^+ is constant. In this case, instead of equation (4.9), we get

$$\frac{d^2n}{ds^2} = -\frac{Kn}{T_g^3}\bar{\nu}_{io}(T_g) + \frac{1}{2}K'\frac{n^2}{T_g} - \frac{1}{s}\frac{dn}{ds} - \frac{5}{2}\frac{1}{T_g}\frac{dn}{ds}\frac{dT_g}{ds} - \frac{n}{4}\left(\frac{1}{T_g}\frac{dT_g}{ds}\right)^2. \tag{4.10}$$

The key term in this equation is the last one on the right side. If the gas heating is small, this term is small everywhere and the profiles which satisfy the boundary condition are merely broadened. For large gas heating and large n_o, the first three terms on the right side of (4.10) are dominant on the axis, and the first term quickly drops out as we move away from the axis. Then, the second and fourth terms cause the profile to turn upwards until the last term predominates to cause a downturn. After the grad n becomes negative, the fourth term helps the last term to steepen the profile toward the wall. Very near the wall the fourth term predominates.

Physically, there are three processes which govern the shape of the electron density profile: ionization, ordinary diffusion, and thermal diffusion. Ionization tends to make the profile convex upwards. Thermal diffusion is represented by the second and last terms on the right side of (4.10). Hence, it tends to make the profile concave upwards near the axis and convex upwards near the wall. The third term is associated with the radial decrease of the ambipolar diffusion coefficient due to increasing gas density. It tends to steepen the profile either upwards or downwards, whichever the case may be.

Now, since the positive ion mobility varies with the gas temperature in the way assumed by the author, the radial decrease of the ambipolar diffusion coefficient is less than the decrease in the work of Ecker and Zöller. Hence, the downturning tendency of the profile is too small, and doubly peaked profiles should not occur.

CHAPTER V

THE POSITIVE COLUMN DOMINATED BY INELASTIC COLLISIONS

In this case the radial electron temperature variation is small, and the left side of (3.16) can be neglected. Also we set $T = T_o$ in the first and third terms on the right side of (3.16). The second term is neglected as usual. It is also true that $T_g/T \ll 1$.

The energy balance equation then becomes

$$e E_{sz}^2 \mu_o k n T_g = n c' \frac{2m}{M} \frac{T_o}{T_g} + \frac{n}{kT_g} \sum_e V_e \bar{\nu}_{eo}(T). \qquad (5.1)$$

If the gas pressure is low enough and the gas heating is not excessive, then the inelastic collisions dominate the energy balance all the way to the wall. In order that inelastic collisions control the energy balance in equation (5.1), it is necessary that

$$\frac{2m}{M} c'T \ll \frac{1}{k} \sum_e V_e \bar{\nu}_{eo}(T) .$$

In the case where $\nu_o = \sigma v$ (σ is a constant cross-section),

$$c' = (4\sigma/\sqrt{\pi}) \sqrt{k/m}\ T^{1/2} .$$

The variation of the inelastic collision term is given by (5.4), so the inequality becomes

$$8\sigma (m/M) \sqrt{k/m\pi}\ T^{3/2} \ll (b/k) \exp.(-\bar{V}_e/kT) .$$

A more definite condition is that the rate of change of the left hand term with respect to T be less than the rate of change of the right hand term with respect to T. This gives the inequality

$$12\sigma(m/M)\sqrt{k/m\pi}\ T^{5/2} < \frac{b\bar{V}_e}{k^2}\ \exp.(-\bar{V}_e/kT).$$

In the case of helium gas,

$$\sigma = 5.65 \times 10^{-16}\ \text{cm.}^2,$$

$$\bar{V}_e \cong 20\ \text{eV.} = 3.2 \times 10^{-11}\ \text{ergs},$$

$$m/M = 1/7350,$$

$$b = 16.3 \times 10^{-20}\ \text{ergs cm.}^3/\text{sec.}$$

Then, for equality of the above terms,

$$T = 24{,}000^{\circ}\ \text{K.}$$

What is the value of R' corresponding to this transition temperature? In the simplest case there is no gas heating, and we assume that the ionization rate is given by equation (5.12) for complete second stage ionization. Then, the particle balance equation (3.18) reduces to

$$(kT_g)^2 \nabla_s^2 n = -(e\bar{v}_{io}/kT\mu_o^+)n.$$

In cylindrical geometry,

$$(e\bar{v}_{io}/kT\mu_o^+)^{1/2} = kT_g \frac{2.4}{R'}.$$

For helium the constants in (5.12) are

$$b_i = 5.1 \times 10^{-9}\ \text{cm.}^3/\text{sec.},$$

and

$$\mu_o^+ \cong 8.5 \times 10^{22}\ \text{gm.}^{-\frac{1}{2}}\text{cm.}^{-3/2},$$

for atomic ions. Then for an electron temperature of 24,000° K., we get

$$R' = 4{,}150 \text{ dyne/cm.} = 3.11 \text{ cm.mm.Hg.}$$

If there is only direct ionization, then $\bar{\nu}_{io}$ is given by equation (5.10), and for $T = 24{,}000^{\circ}$ K.,

$$\bar{\nu}_{io} = 2.30 \times 10^{-14} \text{ cm.}^3/\text{sec.}$$

and

$$R' = 11.9 \text{ cm. mm. Hg.}$$

These values of R' are very small by comparison with the values at which volume recombination becomes important in helium (see Chapter VI).

With the elastic loss term neglected in (5.1), we obtain the equation,

$$\sum_e V_e \bar{\nu}_{eo}(T) = e\mu_o (E_{sz} kT_g)^2. \tag{5.2}$$

Since E_{sz} is assumed to be constant, the energy loss rate term in (5.2) is proportional to T_g^2. Hence, the energy loss rate off the axis is related to that on the axis by the equation,

$$T_{go}^2 \sum_e V_e \bar{\nu}_{eo}(T) = T_g^2 \sum_e V_e \bar{\nu}_{eo}(T_o) . \tag{5.3}$$

If one assumes the electron energy distribution to be Maxwellian, and makes use of empirical curves[27,28] for the $\nu_{eo}(v)$, one finds that the sum of the inelastic collision energy losses can be expressed quite well by the formula,

$$\sum_e V_e \bar{\nu}_{eo}(T) = b \exp.(-\bar{V}_e/kT), \tag{5.4}$$

where $\bar{V}_e$ is the average effective excitation energy. The constant b also contains such an average. Then, (5.3) becomes

$$(T_{go}/T_g)^2 = \exp.\left[\frac{\bar{V}_e}{k}\left(\frac{1}{T} - \frac{1}{T_o}\right)\right], \tag{5.5}$$

or

$$\frac{1}{T} - \frac{1}{T_o} = 2(k/\bar{V}_e)\,\mathrm{Log}\,(T_{go}/T_g). \qquad (5.6)$$

We now analyze the effect of the electron temperature radial variation on the electron density profile. Consider again the case where

$$\nu_o = \sigma\nu \; ; \; \sigma = \text{const.} \qquad (5.7)$$

Then, from the expression (2.11) one obtains the equation,

$$\mu_o = \frac{2e}{3\sigma kT\rho\sqrt{\pi}} = \frac{e2^{3/2}}{3\sigma}(\pi km)^{-1/2}T^{-1/2}. \qquad (5.8)$$

If we insert this expression and the relation (4.6) for D_o into (3.18), we obtain

$$\nabla_s^2 n = -\frac{n}{K}\frac{\bar{\nu}_{io}(T)}{T_o}(T_{go}/T_g)^{3/2} - \frac{1}{2}\nabla_s n \cdot \frac{\nabla_s T_g}{T_g}, \qquad (5.9)$$

where $K = (\sigma k^3/e)\,T_o T_{go}^{3/2}$.

To obtain the variation of the ionization frequency in (5.9), consider two extreme cases:

(1) All ions are formed by direct ionization of unexcited atoms by electron impact, and the ionizing frequency is given quite well by the equation,

$$\bar{\nu}_{io}(T) = \text{const.} \times \exp.(-\bar{V}_i/kT). \qquad (5.10)$$

(2) Nearly all excitations result either directly or indirectly in ionization.

In the second case most of the ionization goes in two steps:

(1) Ground state atoms are either excited or ionized by elec tron impact.

(2) The excited atoms are ionized by electron impact before they can decay permanently to the ground state.

The success of the second stage depends on how long the excited states can be preserved. Experiments[29] indicate that even for small electron densities, the ionization of metastable atoms is important. However, the higher lying excited states often descend quickly to the ground state. For values of pressure times radius of interest here, the resonance radiation thus emitted is almost completely trapped--the excited state wanders a small distance from the place of origin before descending by an alternate route to a metastable state.[30] There is also some production of molecular ions by atomic impact according to the equation,

$$X^* + X \longrightarrow e + X_2^+, \tag{5.11}$$

where the asterisk indicates an excited atom.[31] Hence, the second case applies, and the ionizing frequency is given approximately by

$$\bar{\nu}_{io}(T) = b_i \exp(-\bar{V}_e/kT). \tag{5.12}$$

According to (5.5) the radial variation of $\bar{\nu}_{io}(T)$ is given by

$$\bar{\nu}_{io}(T) = b_i \exp(-\bar{V}_e/kT_o) \times (T_g/T_{go})^2. \tag{5.13}$$

Then, in cylindrical geometry, equation (5.9) becomes

$$\frac{1}{s}\frac{d}{ds}\left(s\frac{dn}{ds}\right) + \frac{1}{2}\frac{d}{ds}(\log T_g)\frac{dn}{ds} = -BnT_g^{1/2}, \tag{5.14}$$

where $$B = (b_i/kT_o)T_{go}^{-1/2}\exp.(-\bar{V}_e/kT_o).$$

If we let $p = s\, dn/ds$, we get the first order equation,

$$\frac{dp}{ds} + p\frac{d}{ds}(\log T_g^{1/2}) = -BsnT_g^{1/2}, \tag{5.15}$$

with boundary condition $p(0) = 0$.

To get an exact solution of (5.15), it is necessary to also solve the gas heating equation simultaneously. However, the parabolic equation,

$$T_g = T_{go}(1 - hs^2), \tag{5.16}$$

is a good approximation to insert into (5.15). Also, n in the source term on the right side of (5.15) is approximated by the parabolic equation,

$$n = n_o(1 - cs^2). \tag{5.17}$$

As Spenke's work shows, a given error in such an approximation should cause much less error in the derivation of the radial profile of n. The solution of (5.15), using the above approximations, is

$$p = -Bn_o T_{go}^{1/2} \frac{s^2}{2(1-hs^2)^{1/2}} \left[1 - (h+c)\frac{s^2}{2} + hc\frac{s^4}{3}\right]. \tag{5.18}$$

This equation can be integrated in a straight forward manner to obtain

$$\frac{n - n_s}{n_o} = -U\left[1/2\,(c/3h - 1)(1-hs^2)^{1/2} + 1/6\,(c/3h-1)(1-hs^2)^{3/2} - \frac{c}{15h}(1-hs^2)^{5/2} + 2/3 - 7c/45h\right]; \quad U = BT_{go}^{1/2}/2h. \tag{5.19}$$

At the tube boundary ($s = R'$) it is assumed that $n = 0$ and $T_g = T_w$, a constant wall value of temperature. Then,

$$c = 1/R'^2, \quad h = \frac{T_{go} - T_w}{R'^2 T_{go}}, \quad \frac{c}{h} = \frac{T_{go}}{T_{go} - T_w}, \tag{5.20}$$

and U is evaluated by applying the wall condition to (5.19). In the special case where $T_{go} \gg T_w$, (5.19) reduces to

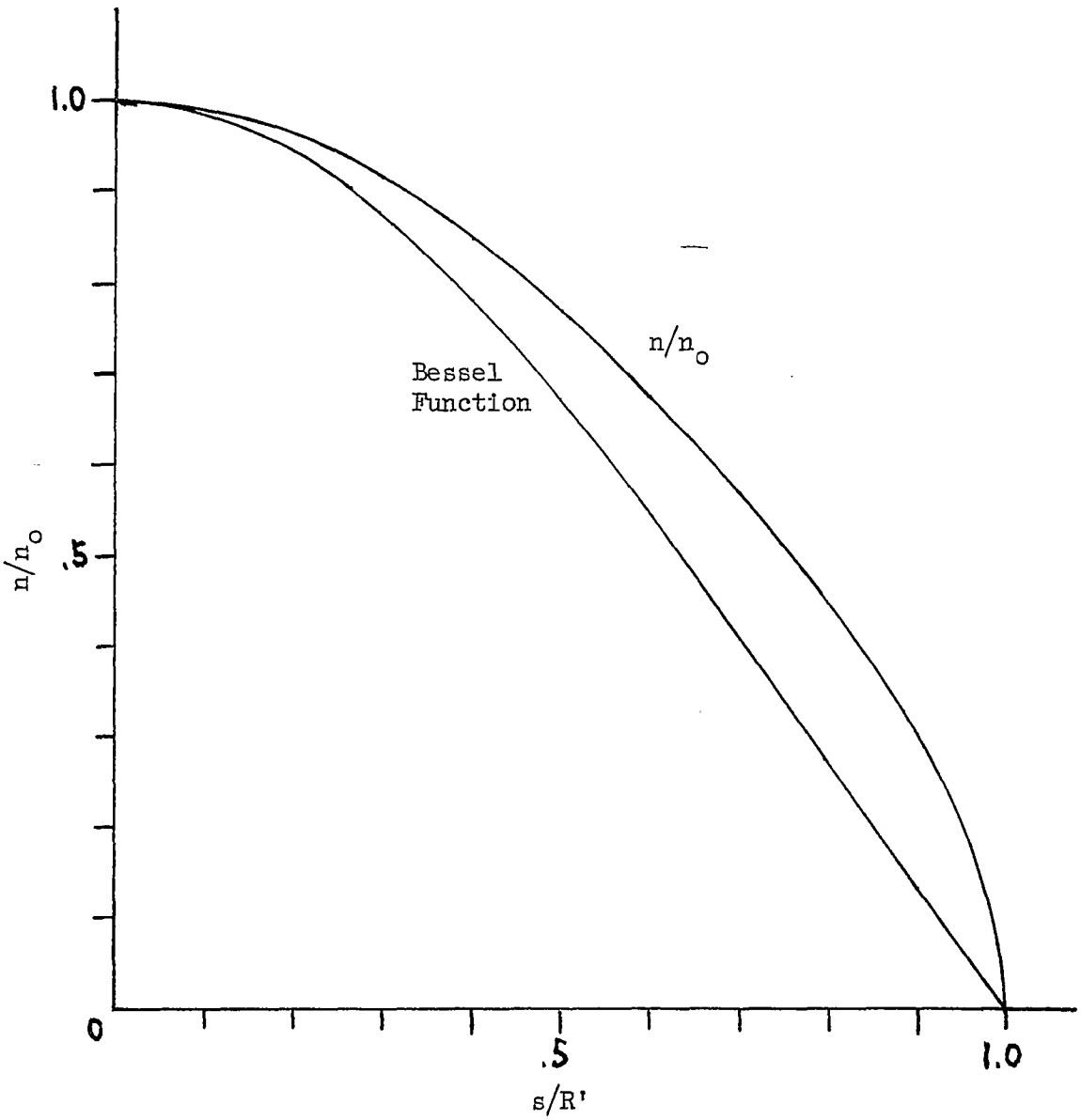

Figure 1. RADIAL PROFILE OF n/n_o IN THE COLUMN DOMINATED BY INELASTIC COLLISIONS

$$\frac{n - n_o}{n_o} = -\left\{ 1 - \frac{15}{23}(1 - s^2/R'^2)^{1/2} \times \right.$$

$$\left. \times \left[1 + \frac{1}{3}(1 - s^2/R'^2) + \frac{1}{5}(1 - s^2/R'^2)^2 \right] \right\} . \qquad (5.21)$$

The resulting variation of n/n_o is shown in Figure 1, where it is compared with the normal Bessel function profile. This comparison shows that even in the extreme case, the broadening of the electron density profile is small. We also see from the solution (5.19) and the constants (5.20) that the shape of the profile is not directly altered by changing R'.

CHAPTER VI

THE POSITIVE COLUMN WITH GAS HEATING AND VOLUME RECOMBINATION

There are several types of situations that may arise where volume recombination is important. Most of these have already been dealt with. The simplest case[7] involves ionization and volume recombination between electrons and positive ions in a gas of uniform density. In this case, the quadratic variation of recombination rate with electron density causes it to decrease faster than the ionization rate. As a result, the net electron production rate per electron increases toward the wall, and the electron density profile is broader than a Bessel function.

More complicated situations arise in electronegative gases, where volume recombination occurs between positive and negative ions for sufficiently large currents.[8-10]

The case of interest here is a heated inert gas containing electrons, atomic ions, and molecular ions of the parent gas. We assume there is no convection. According to experimental data on recombination rates, it is assumed that the dominant process is dissociative recombination of electrons with molecular ions.[32-34] The latter are formed primarily by two processes:

(1) The Hornbeck-molnar process (5.11)[31];

(2) The three-body collision,

$$X^+ + 2X \longrightarrow X + X_2^+. \tag{6.1}$$

Experimental results[35] indicate that the latter process predominates at the pressures of interest for the constriction. Hence, the particle conservation equations for the three charged components are

$$\nabla_r \cdot \underline{\Gamma} = nN\bar{\nu}_{io} - \bar{\alpha} n n_2^+ , \tag{6.2}$$

$$\nabla_r \cdot \underline{\Gamma}^+ = nN\bar{\nu}_{io} + \gamma N n_2^+ - \beta N^2 n^+ , \tag{6.3}$$

$$\nabla_r \cdot \underline{\Gamma}_2^+ = -\bar{\alpha} n n_2^+ - \gamma N n_2^+ + \beta N^2 n^+ . \tag{6.4}$$

Since the current density is not very small, ambipolar diffusion is assumed as before. That is, we assume

$$\begin{aligned} \Gamma_r &= \Gamma_r^+ + \Gamma_{2r}^+ , \\ n &= n^+ + n_2^+ . \end{aligned} \tag{6.5}$$

The resulting particle flow equations are

$$\underline{\Gamma}_r = -\frac{\mu^+\alpha^+ + \mu_2^+\alpha_2^+}{\mu} \frac{1}{N} \nabla_r (nD_o) , \tag{6.6}$$

$$\underline{\Gamma}_r^+ = -\frac{\mu^+\alpha^+}{\mu} \frac{1}{N} \nabla_r (nD_o) , \tag{6.7}$$

$$\underline{\Gamma}_{2r}^+ = -\frac{\mu_2^+\alpha_2^+}{\mu} \frac{1}{N} \nabla_r (nD_o) , \tag{6.8}$$

where $\alpha^+ = n^+/n$, $\alpha_2^+ = n_2^+/n$, so that $\alpha^+ + \alpha_2^+ = 1$.

The space charge field strength is given by

$$\underline{E}_r = -\frac{1}{\mu_o} \frac{1}{n} \nabla_r (nD_o) . \tag{6.9}$$

The quantities $\bar{\alpha}$ and β are respectively the coefficient of dissociative recombination and the rate coefficient for the three body process (6.1). The second term on the right side of (6.4) gives the rate of dissociation of molecular ions by atomic impact. The coefficient γ is a rapidly varying function of gas temperature and also depends greatly on the dissociation energy of the molecular ion of interest.

To obtain the electron conservation equation, we amend (2.24) by adding to the right side of the equation the term

$$n n_2^+ \overline{\tfrac{1}{2} m v^2 \alpha(v)} ,$$

which stands for the loss rate of energy due to the removal of free electrons. This term, however, will be neglected because in the situations of interest the energy lost by recombination is small as compared to that lost either by ionization or elastic impact. The chief reason for this is that ionization energies are very large as compared to the energies for which the recombination cross-section is appreciable. This is not true for the average energy lost in an elastic collision between an electron and an atom. However, elastic collisions occur much more frequently than recombinations.

If we again introduce the variable s = pr, we get for the last two particle balance equations (6.3) and (6.4), with the help of (6.7) and (6.8),

$$kT_g \nabla_s \cdot \left[\frac{\mu^+ \alpha^+}{\mu} kT_g \nabla_s (n D_o) \right] = - n \bar{\nu}_{io} - \gamma n_2^+ + \beta N n^+ , \qquad (6.10)$$

$$kT_g \nabla_s \cdot \left[\frac{\mu_2^+ \alpha_2^+}{\mu} kT_g \nabla_s (n D_o) \right] = \bar{\alpha} \frac{n n_2^+}{N} + \gamma n_2^+ - \beta N n^+ . \qquad (6.11)$$

Of course, (6.2) is not independent but is the sum of (6.3) and (6.4) because of charge conservation.

Unfortunately, these equations do not satisfy the similarity principles of the gas-heated positive column without volume recombination. For if we stipulate that n, n^+, $n_2^+ \propto p$, then we find that

$$\frac{\bar{a} n n_2^+}{N} \propto \frac{p^2}{N} = p k T_g ,$$

$$n \bar{\nu}_{ia} \propto p ,$$

but

$$\beta N n^+ \propto N p = p^2 / k T_g .$$

Hence, the explicit pressure dependence of the terms cannot be divided out of the equations (6.10) and (6.11). The immediate signicance of this is that the shapes of the radial profiles of n, n^+, and n_2^+ differ, and these differences vary with gas pressure. The fact that the rate of conversion of atomic ions is proportional to the square of the gas density[35] leads to an important special case at high pressure--the average atomic ion random-walks a very short distance before converting into a molecular ion. Then, the formation rate of the molecular ions is given essentially by the term, $nN\bar{\nu}_{ia}$. Two subcases arise, which are determined by the value of the coefficient γ . If the dissociation energy of the molecular ions is high enough or the axial gas temperature is low enough, the thermal dissociation is very small, and we can neglect the atomic ions entirely ($n = n_2^+$). In the other subcase the relative concentrations of the two kinds of ions is determined at each point by a

local balance between the dissociation rate of molecular ions and the rate of conversion of atomic ions into molecular ions. This latter case has apparently been observed by Kenty[36] in glow discharges in Xenon. Since the dissociation energy of the noble gas molecular ions decreases rapidly with increasing atomic weight, one would expect the former subcase to apply to the lighter noble gases. This subcase will now be considered.

In addition to the special approximations made for this case, we also use the assumption of Chapter IV--the energy balance is dominated by elastic collisions, so the energy balance equation (4.1) is used. If it is inserted into the gas-heating equation (3.19), the equation,

$$\lambda \nabla_s^2 T_g + \nabla_s T_g \cdot \nabla_s \lambda = - e\mu_o E_{sz}^2 n k T_g / p \,, \qquad (6.12)$$

is obtained. This is one equation in the three unknowns n, T, and T_g. Another is the particle balance equation.

Under the assumption that $n = n_2^+$, one gets from (6.2), with the help of (6.6), the equation,

$$\nabla_s \cdot \left[\frac{\mu_2^+}{\mu} k T_g \nabla_s (n D_o) \right] = - \frac{n \bar{\nu}_{io}}{k T_g} - \frac{\bar{\alpha} n^2}{p} \,. \qquad (6.13)$$

The third equation is (4.1), which can be solved for T in terms of T_g, and this solution is then inserted into (6.13).

The explicit pressure dependence of some terms in (6.13) and (6.12) can be removed by defining the "reduced electron concentration",

$$n' = n/p. \qquad (6.14)$$

For convenience we also designate E_{sz} as E'. The equations (6.12) and (6.13), then, are two simultaneous equations in the variables n' and T_g

with the parameter E', the value of which depends on the values of R' and n_o'.

Consider again the case where the momentum transfer frequency for elastic collisions is proportional to electron velocity (It applies to helium gas for the electron temperatures of interest.). Also assume that

$$\mu_{2o}^{+} = \mu' T_g^{-1/2} , \tag{6.15}$$

$$\lambda = \lambda' T_g^{1/2} , \tag{6.16}$$

$$\bar{\alpha} = \alpha' T^{-3/2} , \tag{6.17}$$

where μ', λ', and α' are constants determined by experiment. The first two assumptions are idealizations. The experimental variation of the molecular ion mobility may be somewhat faster than the variation given by (6.15). The variation of λ given by (6.16) is a little slower than the true variation.[38] The dependence of the dissociative recombination coefficient $\bar{\alpha}$ on the electron temperature was determined by observing the variation of the intensity of emission of recombination radiation with electron temperature in a microwave cavity.[34] Microwave heating was used to vary the electron temperature over a narrow range of 300° K. to 1200° K. The equation (6.17) is also one of three cases in the theory of Bates.[40] The value of the constant λ' was obtained from Chapman and Cowling[41], while the value of μ' was obtained by setting T_g = 300° K. in the data of Chanin and Biondi.[37] The value of the dissociative recombination coefficient in helium is very uncertain. Careful mathematical analysis[43,44] of the experimental conditions of

measurements of electron-ion recombination in helium indicate that the values of the dissociative recombination coefficient deduced by Biondi and others are too high.[32,34,43] They also differ too much. The value at 300° K. obtained by Chen et al[34] is 0.89 x 10^{-8} cm.^{3}/sec. as opposed to 1.7 x 10^{-8} cm.^{3}/sec. deduced by Biondi and Brown.[32,45] Using their analysis of the experimental results, Gray and Kerr[42,43] obtained a new value of the dissociative recombination coefficient in helium of 1.3 x 10^{-9} cm.^{3}/sec. However, the author, using the same analysis, obtained an approximate value of about 6 x 10^{-9} cm.^{3}/sec. Oskam and Mittelstadt in a similar type of analysis[44] fixed the upper limit of the dissociative recombination coefficient at 4 x 10^{-9} cm.^{3}/sec., and this value was used by the author in determining α' in equation (6.17).

As before, we assume complete second stage ionization, and hence,

$$\bar{\nu}_{io} = b_i \exp.(-\bar{V}_e/kT). \tag{6.18}$$

For the case where $\nu_o = \sigma v$, the coefficients c' and μ_o are given by

$$c' = 2m\sigma(2k/m)^{3/2}(\pi k)^{-\frac{1}{2}} T^{\frac{1}{2}},$$

$$\mu_o = (2e/3\sigma k)(2k/m\pi)^{\frac{1}{2}} T^{-\frac{1}{2}}.$$

If these expressions are inserted into (4.1), one gets a quadratic equation in T_g or T, whose solution is

$$T = AT_g, \tag{6.19}$$

where $$A = \tfrac{1}{2}\left[1 + (1 + BE'^2)^{\frac{1}{2}}\right], \text{ and } B = 1/3(e/\sigma)^2(M/m). \tag{6.20}$$

Then, the ionization frequency is given by

$$\bar{\nu}_{i_0} = b_i \exp(-V/T_g), \tag{6.21}$$

where

$$V = \bar{V}_e/kA. \tag{6.22}$$

The particular form the particle balance equation (6.13) takes is

$$\nabla_s \cdot \left[T_g \nabla_s (n' T_g^{1/2}) \right] = G n'^2 T_g^{-3/2} - F \frac{n'}{T_g} \exp.(-V/T_g), \tag{6.23}$$

where

$$F = b_i e/\mu' A k^3 \tag{6.24}$$

and

$$G = \alpha' e A^{-5/2}/\mu' k^2. \tag{6.25}$$

Likewise, equation (6.12) assumes the form

$$\nabla_s^2 T_g + \frac{1}{2T_g} (\nabla_s T_g)^2 = -Hn', \tag{6.26}$$

where

$$H = (2/3\sigma\lambda'\pi^{1/2})(eE')^2 (2k/mA)^{\frac{1}{2}}. \tag{6.27}$$

The solution of the equations (6.21) and (6.22) can be simplified by making the additional variable transformation,

$$y = n' T_g^{\frac{1}{2}}. \tag{6.28}$$

In cylindrical geometry the equations finally become

$$\frac{d^2 y}{ds^2} = y T_g^{-5/2} \left[\frac{Gy}{T_g} - F \exp.(-V/T_g) \right] - \frac{1}{T_g} \frac{dy}{ds} \frac{dT_g}{ds} - \frac{1}{s} \frac{dy}{ds}, \tag{6.29}$$

$$\frac{d^2 T_g}{ds^2} = -Hy T_g^{-1/2} - \frac{1}{2T_g} \left(\frac{dT_g}{ds} \right)^2 - \frac{1}{s} \frac{dT_g}{ds}, \tag{6.30}$$

with the boundary conditions:

$$dy/ds = 0 = dT_g/ds \quad \text{at } s = 0, \tag{6.31}$$

and

$$y = 0, \; T_g = T_w \quad \text{at } s = R'. \tag{6.32}$$

However, for analytical purposes we obtain from (6.23) and (6.26) the equation,

$$\frac{d^2n'}{ds^2} = - Fn'T_g^{-5/2} \exp.(-V/T_g) + n'^2 \left(\frac{G}{T_g^2} + \frac{H'}{2T_g}\right) - \frac{2}{T_g} \frac{dn'}{ds} \frac{dT_g}{ds} + \frac{1}{s} \left(\frac{n'}{2T_g} \frac{dT_g}{ds} - \frac{dn'}{ds}\right) . \qquad (6.33)$$

The Results

Because of the difficulty of solving equations (6.23) and (6.24) analytically, they were solved by the Runge-Kutta method[46] on an IBM 1410 computer.[47] The general procedure was as follows: An appropriate value of the parameter E' was chosen and the coefficients G, F, H, and V were calculated from equations (6.20), (6.22), (6.24), (6.25), and (6.27) after the constants σ, $\bar{V}_e$, b_i, α', λ', and μ' were obtained from experimental data (Table I). For each value of E' a range of values of the gas temperature on the axis were chosen. The computer would then integrate radial profiles of n' and T_g respectively for each value of the axial gas temperature. The boundary conditions (6.31) and (6.32) were satisfied simultaneously for each pair of profiles by generating trial profiles for different values of n'(0) until the true value of R' (= Rp) was bracketed with an error of less than 1%. The above procedure was repeated for several values of E'.

Since the effect of gas heating on the constriction is the phenomenon of interest here, a quantity called the constriction factor was defined by the formula

$$C.F. = R' (\nabla_s^2 n'/n')^{1/2}\Big|_{s=0} . \qquad (6.34)$$

For the zeroth order Bessel function, the value of C.F. is 2.405. The value of C.F. is calculated for each correct radial profile integrated by the computer. One can then plot C.F. as a function of R' for each value of E'. However, the results are misleading because R' depends on both the average gas density and the average gas temperature, which varies appreciably with R' for a given value of E'. The initial value, R_i', which a sealed discharge tube has before the discharge is turned on and the gas heated, is more indicative of the average gas density. Table II contains the values of R_i' calculated with the formula,

$$P_i/p = R_i'/R' = 2T_{gi}/R'^2 \int_0^{R'} \frac{s\,ds}{T_g(s)} \quad , \qquad (6.35)$$

where $T_{gi} = 300^\circ$ K. With these values one can make meaningful plots of the variations of C.F. with R_i' for different values of E' as shown in Figure 2.

Of more immediate interest to the experimenter is the variation of C.F. with Ip_i for a given value of Rp_i. That is, if one keeps the tube radius and cold gas pressure constant and varies only the tube current, the constriction factor varies in a way shown in Table III and Figure 3.

The values of Ip_i were calculated for each case from the radial profiles by using a formula derived as follows: The tube current (due almost entirely to electrons) is given by the equation,

$$I = -e \int_0^R 2\pi r \Gamma_z \, dr \quad , \qquad (6.36)$$

where

$$\Gamma_z = n\bar{v}_z = -\frac{\mu_0}{N} n E_z \, .$$

If we again introduce the similarity transformations, $s = pr$, $E_z = pE'$, $n = n'p$, $I' = Ip$, then (6.36) becomes

$$I' = 2\pi e k E' \int_0^{R'} s \mu_0 T_g n' ds . \qquad (6.37)$$

If we insert into (6.37) the previously given expressions for μ_0 and y, we finally get

$$I' = C A^{-1/2} E' \int_0^{R'} s y ds , \qquad (6.38)$$

where A is given by (6.20) and $C = (4e^2/3\sigma)(2k\eta/m)^{\frac{1}{2}}$.

The cold gas values of I' (= I_i') are finally obtained by multiplying the calculated values of I' by the pressure ratios obtained with (6.35).

Analysis of Results

Figures 4 and 5 show that, in addition to the boundary conditions (6.31) and (6.32), the radial profiles of n' all have two points of inflection. In general, these points move closer to each other as either Ip_i or Rp_i decreases. The qualitative features of the radial profiles are governed primarily by the radial variations of three quantities--the ambipolar diffusion coefficient, the ionization rate, and the volume recombination rate. Since the production of ions and electrons by ionization necessitates an increasing concentration gradient, the ionization term (first term in (6.33)) tends to make the density profile convex upwards. For just the opposite reason, the loss of electrons by volume recombination (second term in (6.33)) tends to make the density profile concave upwards. The effectiveness of these two processes increases with gas density as shown by the factors $T_g^{-5/2}$ and

TABLE I

VALUES OF E/p AND THE CORRESPONDING VALUES OF THE COEFFICIENTS V, A, F, G, AND H
(The values of the empirical constants are shown at the bottom of the table.)

E' (statv. cm./dyne)	A	V (deg.)	F ($deg.^{5/2} cm.^2/dyne^2$)	G ($cm.^3 deg.^3/dyne$)	H ($cm.^3 deg./dyne$)
1.0×10^{-7}	2.654	8.666×10^{4}	1.513×10^{5}	1.966×10^{-8}	5.816×10^{-16}
1.5×10^{-7}	3.682	6.247×10^{4}	1.090×10^{5}	8.672×10^{-9}	1.111×10^{-15}
2.1×10^{-7}	4.928	4.667×10^{4}	8.147×10^{4}	4.185×10^{-9}	1.882×10^{-15}
3.0×10^{-7}	6.805	3.380×10^{4}	5.900×10^{4}	1.868×10^{-9}	3.269×10^{-15}

$\mu' = 2.32 \times 10^{24}$ $deg.^{\frac{1}{2}} gm.^{-\frac{1}{2}} cm.^{-3/2}$, $\lambda' = 891$ gm. cm./$sec.^3 deg.^{3/2}$, $V_e = 19.75$ eV.

$\alpha' = 2.08 \times 10^{-5}$ $cm.^3 deg.^{3/2}/sec.$, $\sigma = 5.65 \times 10^{-16}$ $cm.^2$, $b_i = 5.10 \times 10^{-9}$ $cm.^3/sec.$

TABLE II

VALUES OF Rp, Rp_i, AND THE CONSTRICTION FACTOR C.F. CORRESPONDING TO VALUES OF THE AXIAL GAS TEMPERATURE FOR SEVERAL VALUES OF E/p (p_i is the pressure of the cold gas before the discharge is turned on.)

$E' \times 10^7$ (statv. cm./dyne)	T_{go} (deg. K.)	$R' \times 10^{-6}$ (dyne/cm.)	$R_i' \times 10^{-6}$ (dyne/cm.)	C.F.
1.0	4000	38.0	7.99	7.95
	4250	20.2	4.06	7.39
	4500	11.5	2.22	6.91
	4750	6.97	1.30	6.53
	5000	4.45	.801	6.19
	5500	2.06	.345	5.55
	6000	1.09	.171	5.10
1.5	2750	37.0	10.0	6.42
	3000	14.7	3.75	5.92
	3250	6.75	1.64	5.48
	3500	3.48	.803	5.09
	4000	1.20	.251	4.52
	4500	.527	.102	4.08
2.1	2000	33.1	11.1	5.55
	2100	19.4	6.28	5.34
	2250	9.50	2.94	5.03
	2500	3.53	1.02	4.60
	2750	1.58	.428	4.26
	3000	.816	.208	3.98
3.0	1500	15.2	6.13	4.74
	1750	3.37	1.23	4.29
	2000	1.09	.366	3.91

TABLE III

VALUES OF Ip_i CORRESPONDING TO VALUES OF Rp_i AND E/p

$E' \times 10^7$ (statv. cm./dyne)	$R_i' \times 10^{-6}$ (dyne/cm.)	$I_i' \times 10^{-15}$ (statamp. dyne/cm^2)
1.0	7.99	1.73
	4.06	1.87
	2.22	1.99
	1.30	2.14
	.801	2.29
	.345	2.56
	.171	2.82
1.5	10.0	.956
	3.75	1.05
	1.64	1.17
	.803	1.27
	.251	1.47
	.102	1.66
2.1	11.1	.551
	2.94	.639
	1.02	.720
	.428	.797
	.208	.876
3.0	6.13	.312
	1.23	.368
	.366	.429

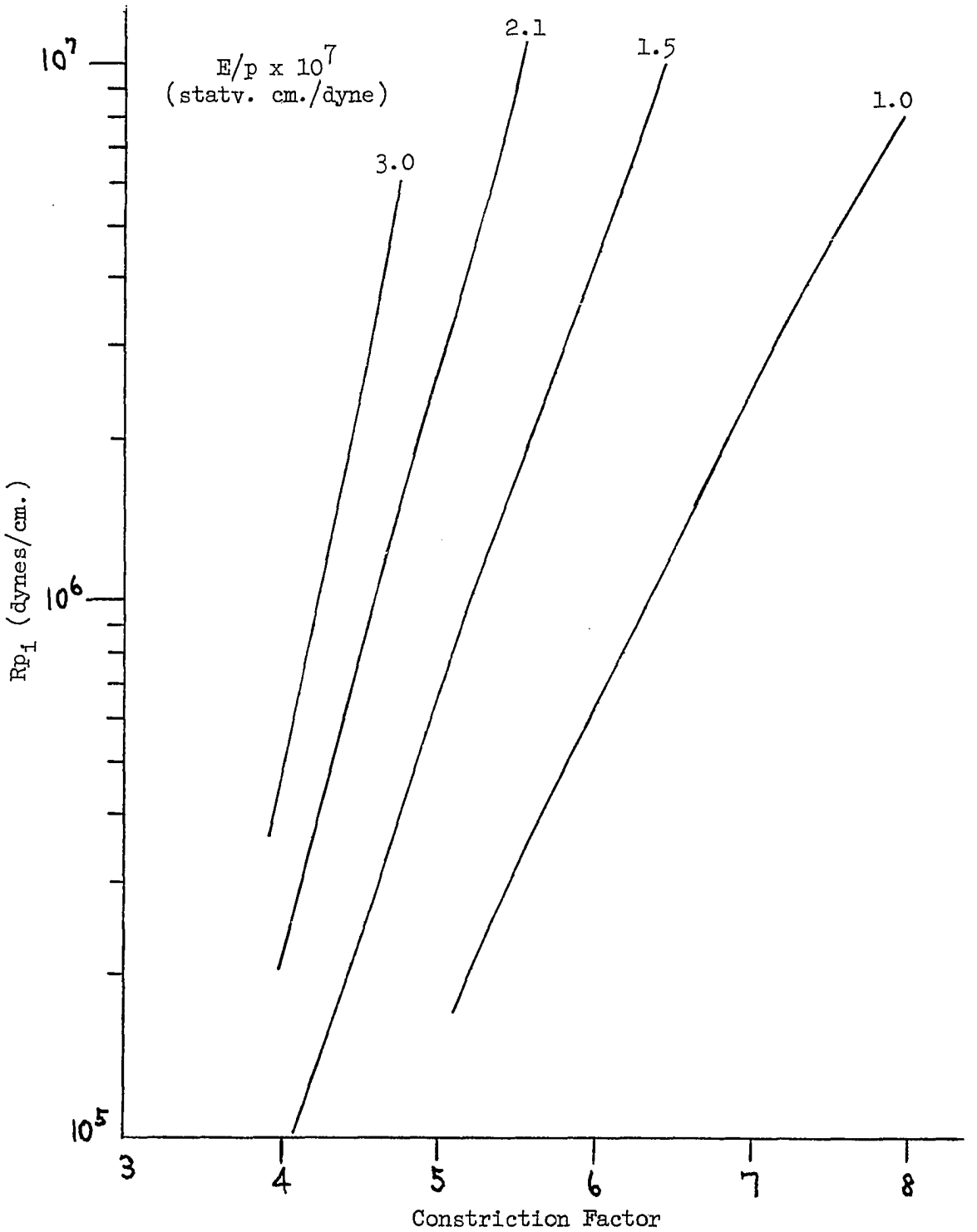

Figure 2. VARIATIONS OF THE CONSTRICTION FACTOR WITH Rp_i FOR SEVERAL VALUES OF E/p (p_i is the pressure of the cold gas before the discharge is turned on.)

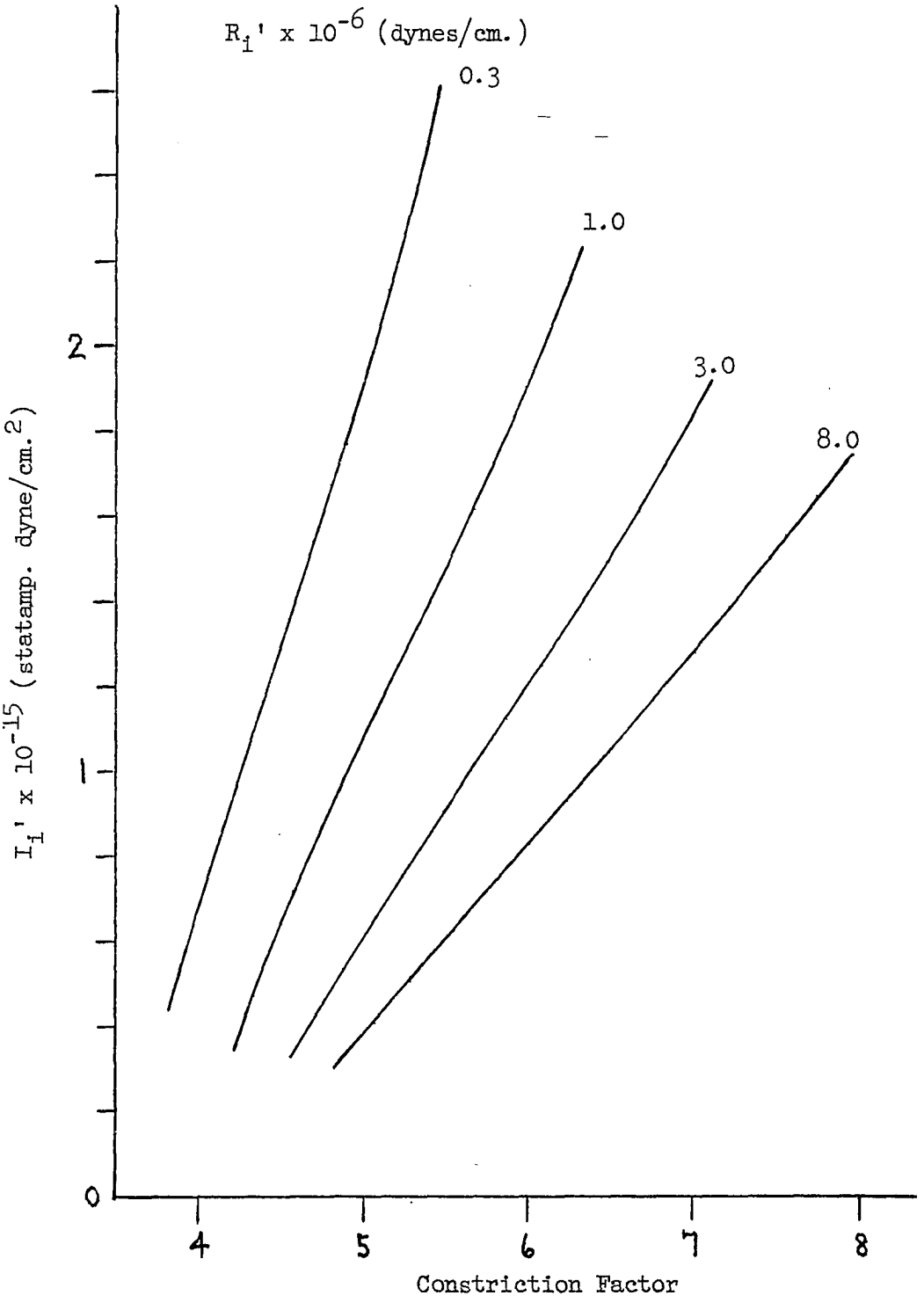

Figure 3. VARIATIONS OF THE CONSTRICTION FACTOR WITH Ip_i FOR SEVERAL VALUES OF Rp_i

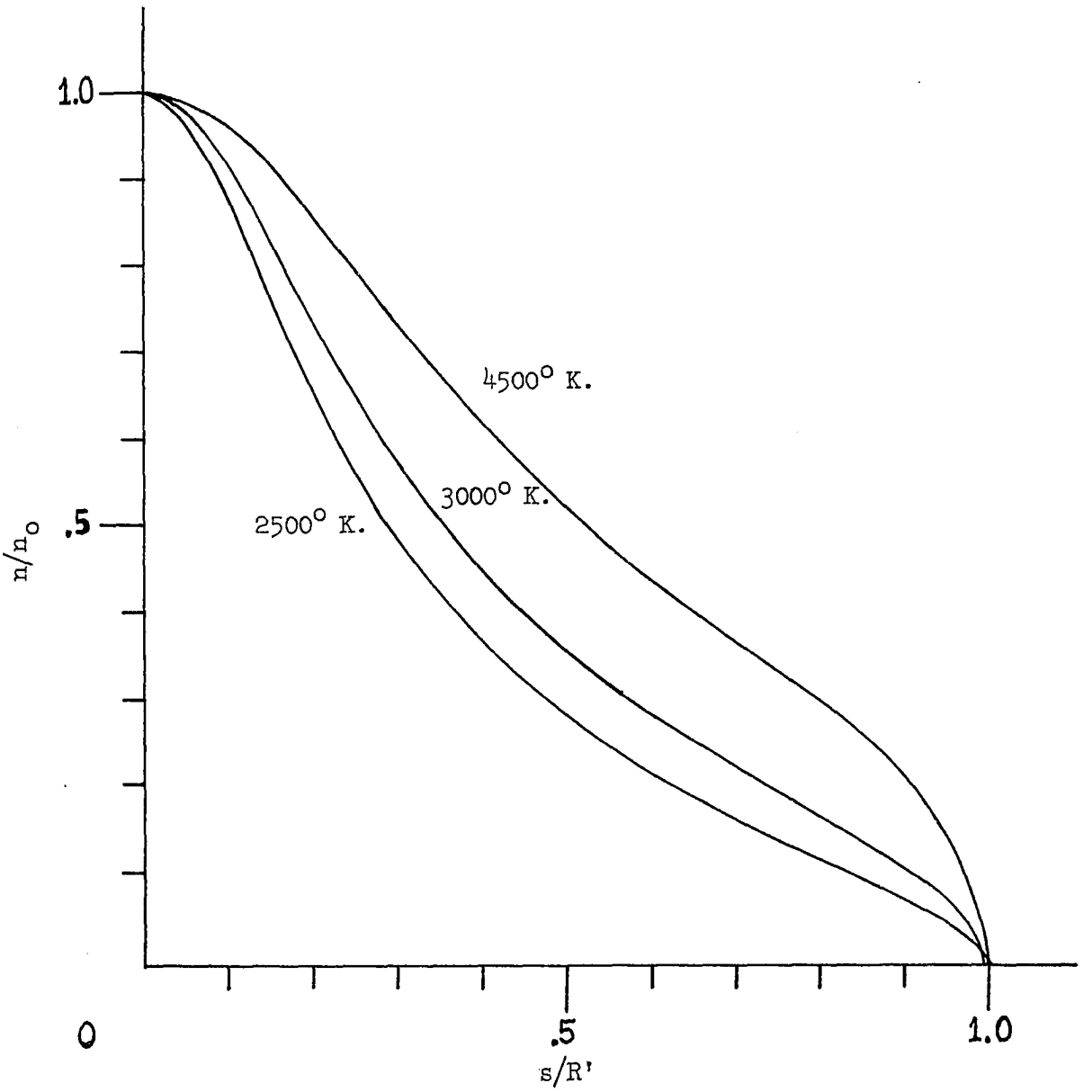

Figure 4. VARIATION OF THE RADIAL PROFILE OF n/n_o WITH AXIAL GAS TEMPERATURE, $E/p = 1.5 \times 10^{-7}$ STATV. CM./DYNE

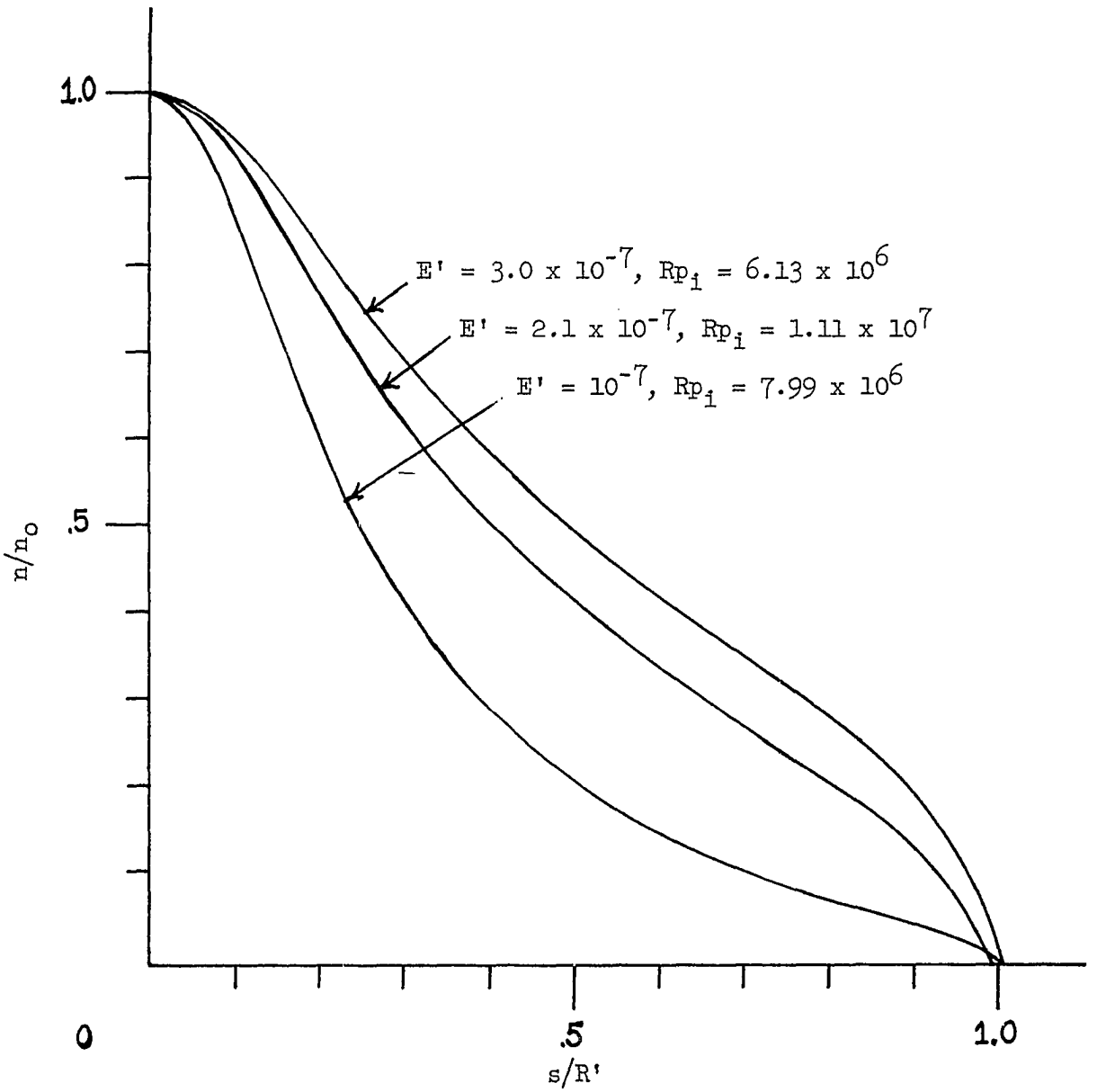

Figure 5. VARIATION OF THE RADIAL PROFILE OF n/n_o WITH E/p
(The values of Rp_i are of the same order of magnitude.)

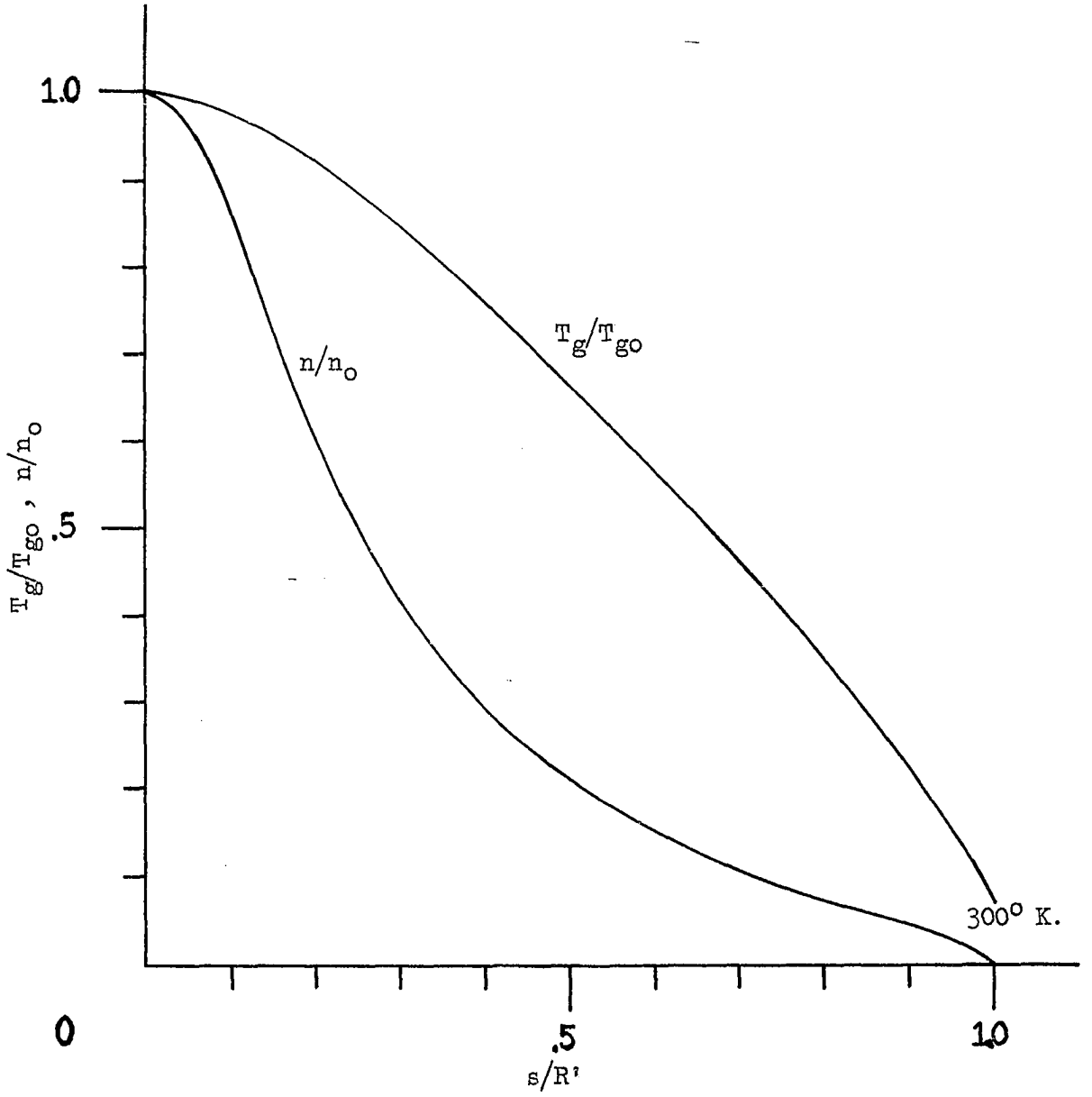

Figure 6. RADIAL PROFILES OF n/n_o AND T_g/T_{go}, $E/p = 10^{-7}$ STATV. CM./DYNE, $T_{go} = 4000°$ K.

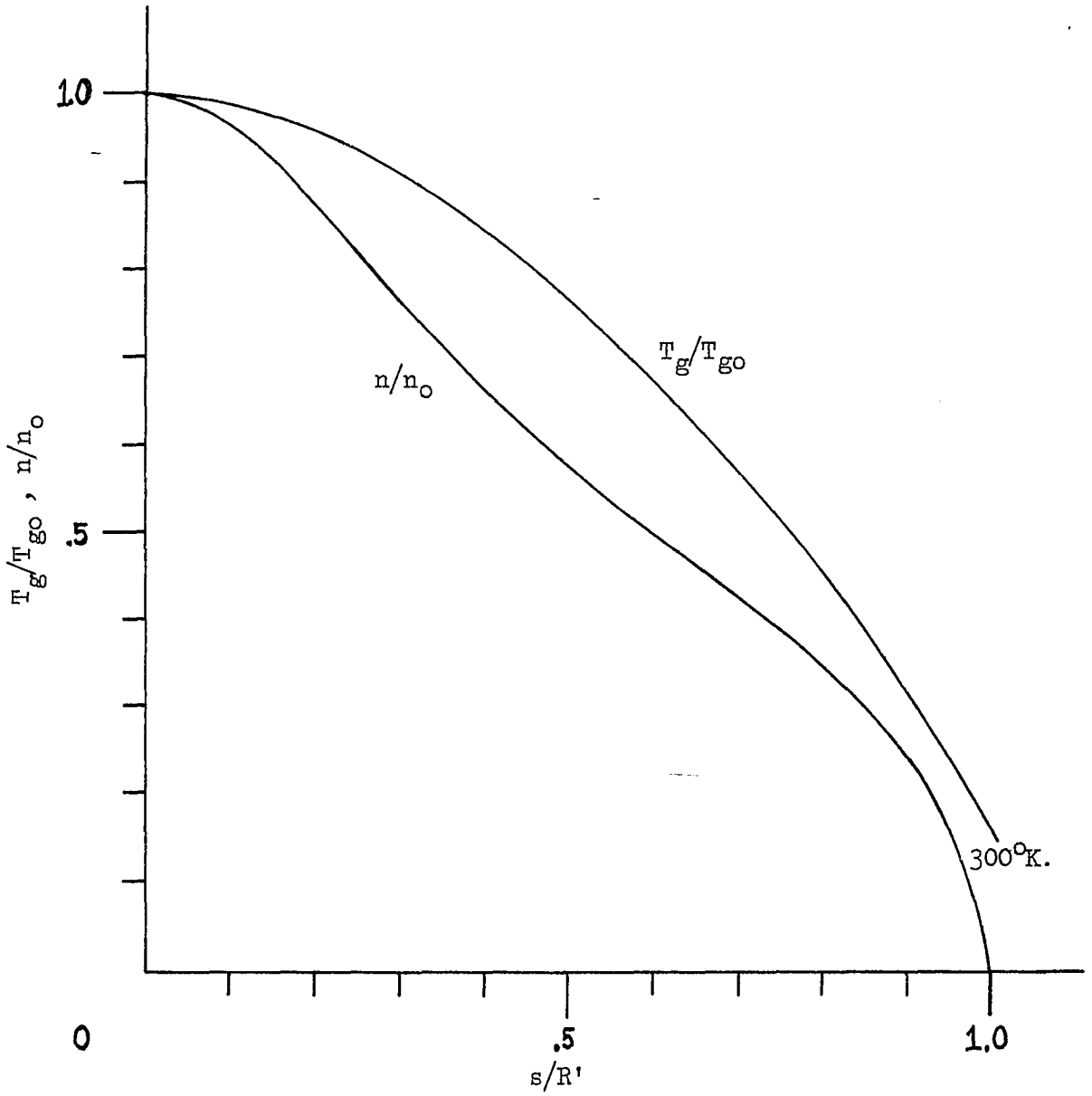

Figure 7. RADIAL PROFILES OF n/n_o AND T_g/T_{go}, $E/p = 3.0 \times 10^{-7}$ STATV. CM./DYNE, $T_{go} = 2000°$ K.

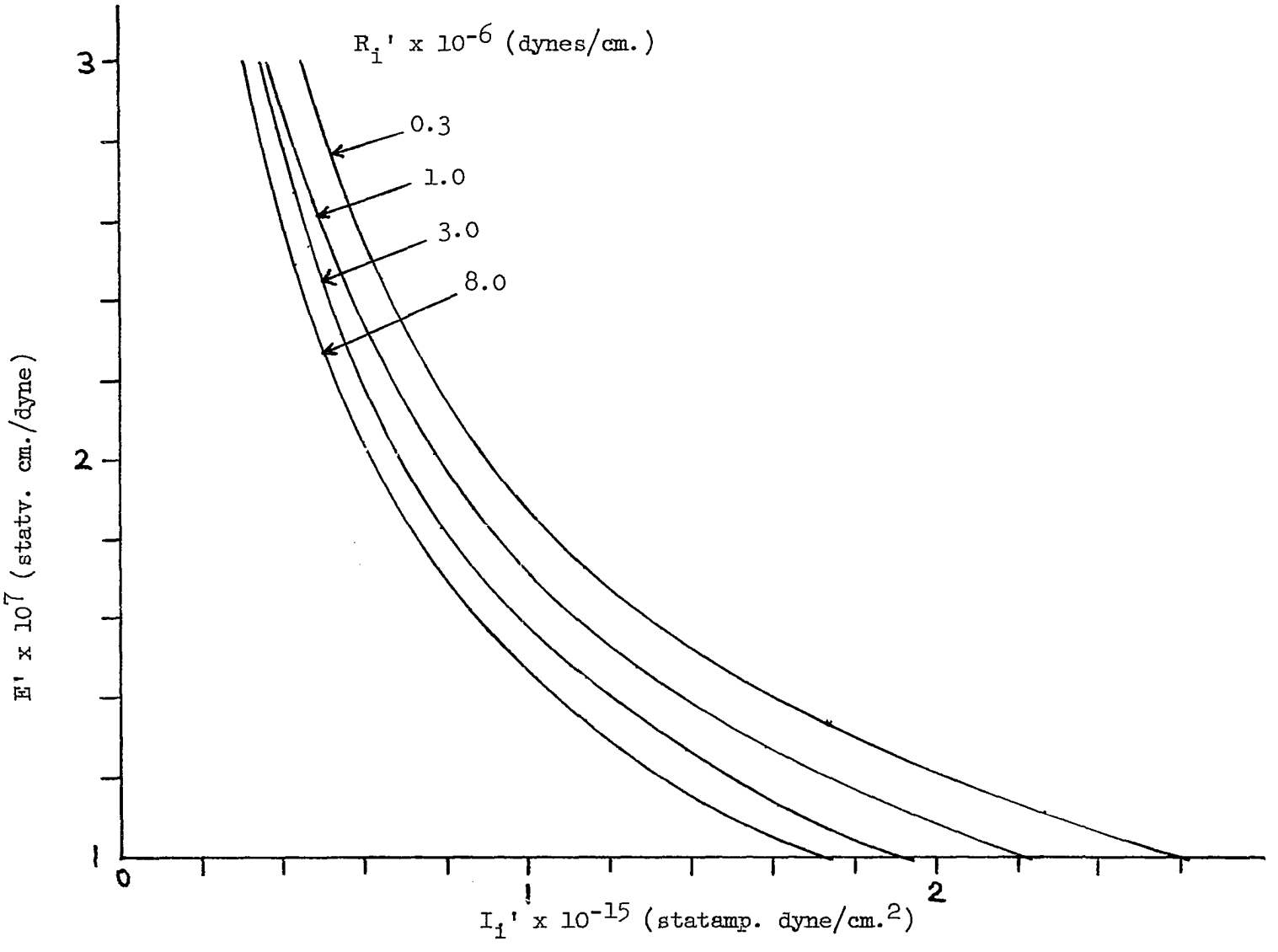

Figure 8. VARIATIONS OF E/p WITH Ip_i FOR SEVERAL VALUES OF Rp_i

T_g^{-3} in (6.33). Because of the gas heating, the radial increase of gas density induces a radial decrease of the ambipolar diffusion coefficient. This in turn necessitates a steepening of the density profile in order to facilitate the required diffusion to the wall. The fourth term in (6.33) most directly shows this tendency, which is to make the density profile broader.

Consider two extreme cases. If both Ip_i and Rp_i are large, the volume recombination rate is an appreciable fraction of the ionization rate on the axis. Also, the radial variation of the gas temperature is relatively great. Hence, the ionization rate decreases very rapidly and leaves the volume recombination process dominant at a relatively short distance from the axis, and the first inflection point is reached. At this point the electron density profile is steep, but the steepening effect of the increasing gas density (fourth term in (6.33)) is still small because $(1/T_g)(dT_g/ds)$ is small (see Figure 6). In fact, this effect stays small because the slope of the density profile rapidly decreases in magnitude as the magnitude of $(1/T_g)(dT_g/ds)$ increases. Since the recombination rate varies quadratically with n', its effect on the profile finally becomes small, and the effect of increasing gas density causes a small downturn near the wall.

In the opposite extreme where Ip_i and Rp_i are both small, the volume recombination rate is less than one tenth as large as the ionization rate on the axis. Because of a smaller gas temperature variation, the radial decrease of the ionization rate is smaller than in the other case. Therefore, the volume recombination rate becomes dominant at a greater distance from the axis. It stays dominant over a shorter

distance because the slopes of the electron density and gas temperature profiles are simultaneously large in the fourth term in (6.33). Physically, this means that as Ip_i and Rp_i are decreased, the volume recombination becomes unimportant and the broadening effect of gas heating progressively sets in. As in the case of gas heating without volume recombination[16], thermal diffusion of electrons (third term in (6.33)) is appreciable. However, its effect is weak. The main reason is that the thermal diffusion term increases more slowly with decreasing gas temperature than does the volume recombination term. We make calculations for two extreme cases with the use of Table I. For our most constricted result,

$$E' = 1.0 \times 10^{-7} \text{ statv. cm./dyne},$$

$$T_{go} = 4000^{\circ} \text{ K}.$$

Then we get $G/T_{go}^3 = 3.07 \times 10^{-19}$,

$$H/2T_{go} = 7.28 \times 10^{-20}.$$

Not only is the recombination term larger on the axis, but it grows much faster toward the wall because of the large gas temperature variation. For the least constricted result,

$$E' = 3.0 \times 10^{-7} \text{ statv.cm./dyne},$$

$$T_{go} = 2000^{\circ} \text{ K}.$$

In this case we get $G/T_{go}^3 = 2.34 \times 10^{-19}$,

$$H/2T_{go} = 8.18 \times 10^{-19}.$$

The thermal diffusion term is important for some distance toward the wall. Evidently, it does not succeed in making the column constrict in this case (Figure 7).

Perhaps, the results of greatest interest to the experimenter

are illustrated in Figure 3. In order to confirm or deny these predictions in the laboratory, one would choose a cylindrical discharge tube having a convenient radius (R = a few cm.) and adjust the helium gas pressure in the tube until Rp_i has one of the values indicated in Figure 3. Several check points could then be chosen on the appropriate curve. At a given check point the required current is calculated by the formula,

$$I = I_i'/p_i.$$

The discharge is started and the tube is either dropped or rotated in order to eliminate convection. After a steady state is reached, the voltage across the tube is varied until the desired current is obtained. To obtain the corresponding constriction factor, it is necessary to take several probe measurements of the electron density in the vicinity of the axis of the discharge. With these measured values the constriction factor,

$$C.F. = R(\nabla_r^2 n/n)^{1/2}\Big|_{r=0},$$

is evaluated by numerical methods.[52]

One can also check the predicted axial gas temperature by measuring the steady state pressure p and comparing p_i/p with the values calculated with (6.35). Since the radial gas temperature variations are approximately parabolic, the equation,

$$T_g = T_{go} - (T_{go} - T_w)(s/R')^2,$$

was inserted into (6.35) to obtain the simple formula,

$$p_i/p = T_{gi}/(T_{go} - T_w) \times \log(T_{go}/T_w). \qquad (6.39)$$

Since in most cases $T_{go} >> T_w$, little error is made by setting

$$T_w = T_{gi} = 300^\circ \text{ K.}$$

Thus, for any point in general on the graphs in Figure 3, one measures the initial pressure p_i, turns on the discharge, measures the steady state pressure p, and solves equation (6.39) for the axial gas temperature T_{go}.

The results of Figure 3 show that the constriction sets in faster with respect to increasing Ip_i for larger values of Rp_i. A possible explanation of this is that for smaller values of Rp_i the greater gas heating makes the broadening effect of the radial variation of the ambipolar diffusion coefficient more important.

The decrease of E/p with increasing Ip_i (Figure 8) is, of course, explained by the fact that as the discharge constricts, the current crowds into the hotter part of the discharge where the electron mobility is greater.

In view of the large amount of gas heating, the assumption that the gas temperature at the tube wall equals the ambient temperature outside the tube may be in error. Since forced cooling outside the tube is feasible, we assume that the temperature of the outer surface of the wall is 300° K. and consider only the conduction of heat through the glass. If the thickness t of the glass wall is small as compared with the tube radius, we get the heat flow equation,

$$Q(R) = -\lambda \left.\frac{dT_g}{dr}\right|_{r=R} \cong \frac{T_w - T_a}{t} \lambda_w , \qquad (6.40)$$

where λ_w is the thermal conductivity of the wall and T_a is the ambient temperature outside the tube. For helium,

$$\lambda = 891 \text{ gm.cm./(sec.}^3\text{deg.}^{3/2}) \times T_g^{\frac{1}{2}},$$

and for glass,

$$\lambda_w = 8 \times 10^4 \text{ gm.cm./(sec.}^3 \text{ deg.)}.$$

Let $$t/R = \text{const.} \equiv C.$$

Then, the similarity rules apply and (6.40) becomes

$$T_w - T_a = -C \frac{\lambda}{\lambda_w} R' \frac{dT_g}{ds} . \tag{6.41}$$

Consider the case where $E' = 1.0 \times 10^{-7}$ statv.cm./dyne and $T_{go} = 4000^\circ$ K. Computer data give

$$dT_g/ds \cong -2.2 \times 10^{-4} \text{ cm. deg.K./dyne},$$

$$R' \cong 3.8 \times 10^7 \text{ dyne/cm.}$$

Then equation (6.41) gives the result,

$$T_w = 300^\circ \text{ K.} + (C \times 1607^\circ \text{ K.}).$$

If $C = 0.1$, then $T_w = 461^\circ$ K. This result is in error since the computer data were obtained for a profile satisfying the boundary condition, $T_w = 300^\circ$ K. However, the error is small because

$$161^\circ \text{ K.} \ll T_{go} - T_w \cong 3540^\circ \text{ K.}$$

Because the fractional error of $T_{go} - T_w$, due to the finite conductivity of the glass, is small, one can make an approximate estimate of the corresponding fractional error in R' with the formula

$$\frac{\Delta R'}{R'} = \frac{T_w - T_a}{R' \times (dT_g/ds)} = -C\lambda/\lambda_w . \tag{6.42}$$

Then, in all cases where $C = 0.1$, the fractional error in R' is about $0.00111 \times T_w^{\frac{1}{2}} \sim .022$.

The constriction factor defined by (6.34) is proportional to R'. However, it also depends on the sharpness of curvature of the profile of

n' on the axis. Hence, as R' decreases, one expects the profile to be narrower, and the constriction factor would tend to remain the same. In all cases, however, the percentage variation of $(\nabla_s^2 n'/n')_{s=0}$ from one trial profile to another is very much less than the corresponding percentage variation of R'. Hence, the percentage errors in the values of the constriction factor in Table II are about the same as the percentage errors of R' in (6.42).

The author does not know of any constriction experiments with helium that are directly related to the theory presented here. However, there is a wealth of experimental data and theory on constrictions in the high pressure D.C. arc, in which thermal equilibrium prevails.[11,51] There are also some observations of constrictions in glow discharges in xenon.[36] The mechanisms proposed by Kenty to explain these constrictions are dissociative recombination and thermal dissociation of the molecular ions by the heated gas. The latter process induces a radial variation of molecular ion concentration. As explained in Appendix III, the radial variation of electron temperature cannot be an important factor in Kenty's observations of the constriction in the low pressure ($\sim$ 10 mm. Hg) xenon discharge.

APPENDIX I

EFFECT OF COULOMB INTERACTIONS ON THE ELECTRON VELOCITY DISTRIBUTION

To estimate the relative importance of random Coulomb interactions in shaping the electron velocity distribution, we will calculate the energy loss rate due to both Coulomb interactions and collisions between electrons and molecules. Since we are concerned here with a weak plasma (specific ionization $< 10^{-5}$), the collision method of treating Coulomb interactions is sufficiently accurate. Hence, we start with a basic formula[48] for the collision rate of change of some quantity ϕ :

$$\frac{\partial(\Delta\phi_1)}{\partial t} = \int (\phi_1' - \phi_1)\, f_2(\underline{v}_2)\, c\, \sigma'(c,\chi)\, d^2\Omega\, d^3\underline{v}_2 \qquad (I.1)$$

In this equation, ϕ_1 is the quantity belonging to the particles no. 1, all having the same velocity $\underline{v}_1$, c is the relative speed $|\underline{v}_1 - \underline{v}_2|$, and $\sigma'(c,\chi)$ is the differential scattering cross-section.

This equation was used by S. Chandrasekhar to analyze the effects of random interactions among stars in stellar systems. Since the gravitational and the Coulomb forces have the same dependence on distance, we can use Chandrasekhar's results by changing only a few constants in his formulas. In plasmas, however, screening of the positive ions by the electrons is sometimes important, and the interactions are weakened. The plasma densities of interest here are low, and therefore the Debye length

(the screening parameter) is large as compared to the average distance between neighboring electrons. Hence, the screening effect is small at that distance, which is therefore used as a cut-off value of the impact parameter: Cut-off value $\equiv a = .554 \times n^{-1/3} \approx \frac{1}{2}n^{-1/3}$.

To estimate the effects of Coulomb interactions on electron energies, we use one of Chandrasekhar's results[50] to get

$$\frac{\partial(\Delta E)}{\partial t} = - \frac{4\pi n e^4}{mv} G(x_0) \operatorname{Log} qv^2, \qquad (I.2)$$

where $$G(x_0) = \frac{1}{2x_0^2}\left[\Phi(x_0) - x_0 \Phi'(x_0)\right],$$

$$x_0 = \beta v, \quad q = ma/2e^2,$$

and $\Phi(x_0)$ is the error integral.

This equation gives the average energy loss rate of a group of electrons having the speed v, mass m, and charge -e.

The corresponding energy loss rate due to collisions with molecules is obtained from the third term of equation (2.24) to get

$$\frac{\partial_c(\Delta E)}{\partial t} = - (m/M)(mv^2 \nu_0 N). \qquad (I.3)$$

Let us consider a representative electron velocity of 10^8 cm./sec. and choose $x_0 = 1$, the value for which $E = kT$. Then $G(x_0) = 0.214$. For the velocities and electron concentrations of interest, $qv^2 >> 1$, and $\log qv^2$ varies very slowly with n. Hence, we assume that $n = 10^{12}/\text{cm.}^3$ and calculate $\log qv^2 = 6.90$. Setting (I.2) equal to (I.3), we obtain for the specific ionization,

$$n/N = 1.16 \times 10^{-22} v^3 \nu_0(v) \qquad (I.4)$$

For $v = 10^8$ cm./sec. in helium, $\nu_o = 5.65 \times 10^{-8}$ cm.^{3}/sec., and $n/N = 6.53 \times 10^{-6}$. This value applies to low pressure glow discharges where the electron temperature is about 30,000° K. In the discharge considered in Chapter VI, the electron temperature is somewhat lower and varies from 10,200° K. on the axis of the coolest discharge to 15,900° K. in the hottest discharge. Consider the worst case presented in the results in Chapter VI:

$E' = 3 \times 10^{-7}$, $T_{go} = 1500°$ K., $y_o = 3.5 \times 10^5$, $R' = 1.525 \times 10^7$.

If we choose R = 3 cm., then, with the variable transformations given in Chapter VI, we obtain on the axis

$$n_o = 4.58 \times 10^{10}/\text{cm.}^3$$

$$N_o = 2.69 \times 10^{19}/\text{cm.}^3$$

$$n_o/N_o = 1.70 \times 10^{-9}.$$

For an electron temperature of 10,200° K., $v^2 = 4.63 \times 10^{15}$ cm.^{2}/sec.^{2}. For this case the value of specific ionization for which the Coulomb interaction is effective is $n/N = 1.34 \times 10^{-6}$, or about three orders of magnitude larger than the calculated value on the axis of the discharge.

The best case in the results of Chapter VI is the case where both E' and R' are smallest. For that case we have $E' = 10^{-7}$, $T_{go} = 6000°$ K., $R' = 1.008 \times 10^6$, $y_o = 3.914 \times 10^9$. Then the actual concentrations on the axis of the discharge are

$$n_o = 1.83 \times 10^{13}/\text{cm.}^3$$

$$N_o = 4.81 \times 10^{17}/\text{cm.}^3$$

$$n_o/N_o = 3.80 \times 10^{-5},$$

and the axial electron temperature is 15,900° K. For these values, the critical value of specific ionization on the axis of the discharge is

$n/N = 4.17 \times 10^{-6}$.

Hence, only some of the more constricted discharges satisfy the condition for strong Coulomb interactions. Since $\gamma_0(v)$ in (I.4) is proportional to v for the electron velocities of interest,

$$n/N \propto v^4 \propto T^2,$$

and there is a rapid radial decrease in the critical value of specific ionization that is at least as fast as the decrease of the actual value. It follows that the condition for strong Coulomb interactions is more likely to be satisfied in the outer parts of the discharge.

APPENDIX II

ELECTRON ENERGY LOSS BY AMBIPOLAR DIFFUSION

In Chapter III it is assumed that the electron energy loss rate due to ambipolar diffusion is negligible. The proof of this is simplified by assuming slight gas heating so that the second term on the right side of (3.16) is the only term generating a radial electron temperature variation. Also, we simplify the analysis even further by assuming that ν_o = const. The inelastic collision energy loss rate is taken to be negligible so that an upper limit of the variation of electron temperature can be found. For ν_o = const., the expressions for the coefficients in (3.16) are

$$\mu_o = e/m\nu_o ,$$

$$D_o = kT/m\nu_o ,$$

$$c = 5/2 ,$$

$$c' = 3/2 \times \nu_o .$$

The axial field strength term can be eliminated from (3.16) by solving for it in terms of the axial values of the other terms. Thus, in view of the above assumptions and approximations, (3.16) becomes

$$A\left[\frac{1}{n_o}\nabla_s\cdot(nT\nabla_s T)\Big|_o - \frac{1}{n}\nabla_s\cdot(nT\nabla_s T)\right] = B(T_o - T) - C\left(\frac{\nabla_s(nT)}{n}\right)^2 , \quad (II.1)$$

where T_o and n_o refer to axial values of T and n, and the constants are given by the formulas,

$$A = \frac{5k^2}{2m\nu_o} \; , \quad B = \frac{3m}{M}\frac{\nu_o}{kT_g^2} \; , \quad C = \frac{\mu_o^+ k^2}{e} \; .$$

If we expand the divergence and gradient terms in this equation, we get

$$A\left[\frac{T_o}{T^2}\nabla_s^2 T\Big|_o - \frac{1}{T}\nabla_s^2 T - \left(\frac{\nabla_s T}{T}\right)^2 - \frac{\nabla_s n}{n}\cdot\frac{\nabla_s T}{T}\right] = \frac{B}{T^2}(T_o - T)$$

$$- C\left[\left(\frac{\nabla_s T}{T}\right)^2 + \left(\frac{\nabla_s n}{n}\right)^2 + 2\frac{\nabla_s n}{n}\cdot\frac{\nabla_s T}{T}\right] . \qquad \text{(II.2)}$$

For large values of Rp the gradient terms are small, so the heat conduction terms on the left side of this equation can be set equal to zero at least near the axis of the discharge. In fact, only two terms may be appreciable, so we get

$$B(T - T_o) = - CT^2\left(\frac{1}{n}\frac{dn}{ds}\right)^2 . \qquad \text{(II.3)}$$

This is a quadratic equation whose solution is

$$T = \frac{B}{2C}\left(-1 + \sqrt{1 + 4T_o\frac{C}{B}\left(\frac{1}{n}\frac{dn}{ds}\right)^2}\right)\left(\frac{n}{dn/ds}\right)^2 . \qquad \text{(II.4)}$$

If T varies little, then, $n = n_o J_o(Ks)$,

and $$-(dn/ds)/n = K\left[J_1(Ks)/J_o(Ks)\right] .$$

If the discharge takes place in helium gas at a pressure of 10 mm.Hg in a tube of radius 2.4 cm., then, the electron temperature should be about 25,000° K. and we get $C/B \sim 1.6 \times 10^{-8}$ cm.^{2}/deg. It follows that the solution for T can be approximated by the equation,

$$T = T_o\left[1 - \frac{C}{B}T_o\left(\frac{1}{n}\frac{dn}{ds}\right)^2\right] , \qquad \text{(II.5)}$$

everywhere except very close to the wall. That is, the electron temperature is nearly constant over almost the entire cross-section. Suppose the exact solution (II.4) of the equation (II.3) is valid near the wall at points close enough to the wall so that

$$4T_0 \frac{C}{B} \left(\frac{1}{n}\frac{dn}{ds}\right)^2 \gg 1 .$$

There the solution can be approximated by the equation,

$$T \approx \frac{n}{dn/ds} \left(\frac{BT_0}{C}\right)^{1/2} . \qquad \text{(II.6)}$$

This can be used to estimate the size of one of the terms neglected in the original equation (II.2). For example,

$$\frac{1}{T}\frac{dT}{ds}\frac{1}{n}\frac{dn}{ds} = \left(\frac{1}{n}\frac{dn}{ds}\right)^2 .$$

Hence, the quadratic equation is not valid near the wall. In our numerical example,

$$C/A = 6.8 \times 10^{-3}.$$

Hence, the leading terms in the equation (II.2) for the region near the wall are probably (II.7)

$$B(T - T_0) = AT\frac{dT}{ds}\frac{1}{n}\frac{dn}{ds} - C\left(\frac{T}{n}\frac{dn}{ds}\right)^2 + A\left(T\nabla_s^2 T - T_0\nabla_s^2 T\Big|_0\right).$$

It appears from this equation that the second term on the right first becomes appreciable and induces a negative temperature gradient. Then the first term on the right quickly grows to partially cancel the effect. The contribution of the other terms on the right is hard to evaluate and may be positive.

The behavior of the electron temperature very near the wall may

be obtained more correctly by neglecting all terms in (II.7) except the first two on the right side. That is, we solve the equation,

$$A \frac{1}{T} \frac{dT}{ds} \frac{1}{n} \frac{dn}{ds} = C \left(\frac{1}{n} \frac{dn}{ds} \right)^2 , \qquad \text{(II.8)}$$

and get the solution,

$$T = T_o \, (n/n_o)^{C/A} . \qquad \text{(II.9)}$$

Since $C/A \ll 1$, the temperature varies little except near the wall.

For larger values of pressure times tube radius, the first term on the right side of (II.2) becomes more dominant, and the solution (II.3) becomes increasingly valid and the radial temperature variation is smaller.

APPENDIX III

TRANSITION FROM THE COLLISION-DOMINATED TO THE CONDUCTION-DOMINATED COLUMN

In Chapter III it was noted that the relative importance of the collision energy loss terms on the right side of the energy balance equation (3.16) increases with R'^2. Hence, over a limited range of values of R', the dominance of the energy balance shifts rapidly from the heat conduction terms on the left side to the elastic collision terms on the right side of (3.16). This statement and the following analysis apply only if the inelastic collision terms have already lost energy dominance at the values of R' of interest.

To compare the relative importance of the elastic collision terms and the heat conduction terms for a given pressure and radius, we take the solution (4.3) of (3.16) for the collision-dominated column and use it to calculate one of the terms on the left side of (3.16). Assume that ν_o = const. Then μ_o and c' are also constant, and

$$T/T_o = (T_g/T_{go})^2. \qquad \text{(III.1)}$$

Also, the energy balance equation reduces to equation (II.2) in Appendix II. With the above solution we get

$$\nabla_s^2 T = (2T_o/T_{go}^2)\left[T_g \nabla_s^2 T_g + (\nabla_s T_g)^2\right], \qquad \text{(III.2)}$$

and $$\nabla_s T = (2T_o / T_{go}^2)\, T_g \nabla_s T_g .$$

Then, the off-axis terms on the left side of equation (II.2) become

$$-2A\left[\frac{\nabla_s^2 T_g}{T_g} + 3\frac{\nabla_s T_g}{T_g} + \frac{\nabla_s n}{n}\cdot\frac{\nabla_s T_g}{T_g}\right],$$

and for the important off-axis term on the right side we get

$$B/T = (BT_{go}^2/T_o)/T_g^2 .$$

The axial values of these terms will be calculated and compared. For T_g assume the function, $T_g = T_{go} - as^2$, with the boundary condition, $T_g(R') = T_w$, so that $a = (T_{go} - T_w)/R'^2$. We now calculate the value of R' at which the heat conduction terms equal the collision term. The result is

$$R'^2 = 8(T_{go} - T_w)\, T_o T_{go}/F,$$

where according to the definitions of A and B in Appendix II,

$$F = 1.2 \times (m/M)(m\nu_o^2/k^3).$$

For helium gas, $F \sim 19.8$.

Then, if $T_o = 25{,}000^\circ$ K. and $T_{go} \gg T_w$, $R' \approx 35.6 \times T_{go}$.

If $T_{go} = 2000^\circ$ K., $R' = 71{,}200$ dyne/cm. = 53.4 cm. mm. Hg.

Evidently, electron heat conduction is negligible for the values of R' at which one would expect recombination to be effective in helium. The above value of R' is an overestimate, because for that value,

$$\nu_o \sim v \times \text{const.}$$

in helium, and the electron temperature varies more slowly with gas temperature than in the case where ν_o = const.

The expression for F shows that in the heavier noble gases

electron heat conduction is more important since the mass ratio is much less. Also, V_o is much less in neon than it is in helium. For the same reasons, the energy loss due to inelastic collisions in the heavier gases also has greater relative importance. At the same time, the volume recombination coefficient is much larger in the heavier noble gases ($> 2 \times 10^{-7}$). Therefore, in the heavier inert gases the value of Rp at which the constriction sets in is determined by the relative importance of either electron heat conduction or inelastic energy loss.

LIST OF REFERENCES

1. Schottky, W., Phys. Z. 25, 342 (1924).

2. Buneman, O., "The Bennett Pinch", pp. 202-224, Plasma Physics, ed. by J. E. Drummond (New York: McGraw-Hill, 1961).

3. Copland, G. E., thesis, University of Oklahoma (1965).

4. Ecker, G., W. Kröll, and O. Zöller, Phys. of Fluids 7, 2001 (1964).

5. Fowler, R. G., Proc. Phys. Soc. 80, 620 (1962).

6. Spenke, E., Zeit. für Physik 127, 221 (1950).

7. Fabrikant, V., Compt. Rend. Acad. Sci. U.S.S.R. 24, 531 (1939).

8. Woolsey, G. A., "Constriction in the Positive Column", p. 141, CR VI Conf. Internat. Phenomenes d'Ionization dans les Gaz, Vol. II (Paris: SERMA, 1963).

9. Ecker, G. and G. Allbrecht, Z. für Naturf. 17A, 848 (1962).

10. Ecker, G. and G. Allbrecht, Z. für Naturf. 17A, 854 (1962).

11. Finkelnburg, W. and H. Maecker, "Elektrische Bögen und Thermische Plasma", pp. 254-440, Handbuch der Physik, Vol. XXII, ed. by S. Flügge (Berlin: Springer-Verlag, 1956).

12. Bennett, S. and J. F. Connors, "Theory and Experiment With a Gas-Stabilized Constricted Arc", pp. 109-118, IEEE Trans. Nuclear Sci. (U.S.A.), Vol. NS-XI, (1964).

13. Jedlicka, J. R. and H. A. Stine, "Axial Flow Through the Wall-Constricted Direct-Current Arc---Comparison of Theory and Experiment", pp. 104-108, IEEE Trans. Nuclear Sci. (U.S.A.), Vol. NS-XI, (1964).

14. Patt, H. J., and G. Schmitz, Zeit. für Physik 185, 1 (1965).

15. Schmitz, G., H. J. Patt, and J. Uhlenbusch, Zeit. für Physik 173, 552 (1963).

16. Ecker, G. and O. Zöller, Phys. of Fluids 7, 1996 (1964).

17. Allis, W. P., "Motions of Ions and Electrons", pp. 383-444, Handbuch der Physik, Vol. XXI, ed. by S. Flügge (Berlin: Springer-Verlag, 1956).

18. Morse, P. M., W. P. Allis, and E. S. Lamar, Phys. Rev. 48, 412 (1935).

19. Holstein, T. R., Phys. Rev. 70, 367 (1946).

20. Margenau, H., Phys. Rev. 73, 297 (1948).

21. Cahn, J. H., Phys. Rev. 75, 293 (1949).

22. Cahn, J. H., Phys. Rev. 75, 838 (1949).

23. See Reference 24, pp. 94 and 95.

24. Druyvesteyn, M. J. and F. M. Penning, Rev. Mod. Phys. 12, 87 (1940).

25. Chapman, S. and T. G. Cowling, The Mathematical Theory of Non-Uniform Gases, 2d Ed., (London: Cambridge University Press, 1952), Chapters 8, 9, 18.

26. See Reference 25, p. 220.

27. Smit, J. A., Physica 3, 543 (1937).

28. Maier-Leibnitz, H., Z. Physik 95, 489 (1935).

29. Meissner, K. W. and W. F. Miller, Phys. Rev. 92, 896 (1953).

30. Fowler, R. G., "Radiation from Low Pressure Discharges", p. 216, Handbuch der Physik, Vol. XXII, ed. by S. Flügge (Berlin: Springer-Verlag, 1956).

31. Hornbeck, J. A. and J. P. Molnar, Phys. Rev. 84, 625 (1951).

32. Biondi, M. A. and S. C. Brown, Phys. Rev. 75, 1700 (1949).

33. Biondi, M. A. and T. R. Holstein, Phys. Rev. 82, 962 (1951).

34. Chen, C. L., C. C. Leiby, and L. Goldstein, Phys. Rev. 121, 1391 (1961).

35. Phelps, A. V. and S. C. Brown, Phys. Rev. 86, 102 (1952).

36. Kenty, C., "Dissociative Recombination and the Constriction of the Positive Column", pp. 356-366, Ionization Phenomena in Gases, Vol. I, ed. by H. Maecker (Amsterdam: North-Holland Publ. Co., 1962).

37. Chanin, L. M. and M. A. Biondi, Phys. Rev. 106, 473 (1957).

38. See Reference 25, p. 223.

39. Bates, D. R., Phys. Rev. 77, 718 (1950).

40. Bates, D. R., Phys. Rev. 78, 492 (1950).

41. See Reference 25, p. 241.

42. Gray, E. P. and D. E. Kerr, Bull. of Am. Phys. Soc. (II) 5, 372 (1960).

43. Gray, E. P. and D. E. Kerr, Ann. of Phys. 17, 276 (1961).

44. Oskam, H. J. and V. R. Mittelstadt, Phys. Rev. 132, 1445 (1963).

45. Biondi, M. A. and S. C. Brown, Phys. Rev. 76, 1697 (1949).

46. Hildebrand, F. B., Introduction to Numerical Analysis (New York: McGraw-Hill, 1956), pp. 233-239.

47. I am indebted to the personnel of the computer laboratory of the University of Oklahoma for processing the program.

48. See Reference 25, p. 62.

49. Chandrasekhar, S., Principles of Stellar Dynamics (New York: Dover Publ. Inc., 1960), Chapter 2.

50. See Reference 49, p. 229.

51. Elenbaas, W., The High Pressure Mercury Vapour Discharge (Amsterdam: North-Holland Publ. Co., 1951), Chapters 2-4.

52. See Reference 46, Chapter 4.

53. Allis, W. P. and D. J. Rose, Phys. Rev. 93, 84 (1954).